Addis Ababa University

Addis Ababa Institute of Technology

African Railway Center of Excellence (ARCE)

Thesis for MSc in Railway Engineering

Civil Infrastructure

A Thesis Submitted to the School of Graduate Studies of Addis Ababa University in Partial Fulfilment of the Requirements for the Degree of Master of Science in Railway Engineering

MODELING AND ANALYSIS OF RAIL PAD STIFFNESS ON BALLASTED RAILWAY TRACK

By

Chebaran Jonex GSR/4374/14

Advisor: **Dr. -Ing. Henok Fikre**

July, 2023
Addis Ababa
Ethiopia

MODELING AND ANALYSIS OF RAIL PAD STIFFNESS ON BALLASTED RAILWAY TRACK

APPROVAL

The undersigned has examined the thesis entitled "**Modeling and analysis of rail pad stiffness on ballasted railway track"** presented by Chebaran Jonex of registration number GSR/4374/14, in partial Fulfillment of the Requirements for the Degree of Master of Science in Railway Engineering (Civil Infrastructure).

Submitted by:

Chebaran Jonex Student	_____ Signature	_____ Date

Approved by:

Henok Fikre (PhD) Advisor	_____ Signature	_____ Date
Mr. Zewdie Moges Internal Examiner	_____ Signature	_____ Date
Biruktawit Taye (PhD) External Examiner	_____ Signature	_____ Date
Mr. Zewdie Moges ARCE Chair	_____ Signature	_____ Date

DECLARATION

I certify that this research work entitled “modeling and analysis of rail pad stiffness on ballasted railway track” is my own work. The work has not been presented elsewhere for assessment. Where material has been used from other sources, it has been appropriately acknowledged/referred.

_____

Chebaran Jonex

DATE:

ABSTRACT

Railway infrastructure**,** has become the most competitive transport means due to its unique advantages (efficiency, transportation capacity, low environmental impact, etc). Rail pad is the regularly used resilient element, and is very crucial as it act as a softening medium between rail and sleeper. A soft rail pad permits a larger rail deflection which lead to the fatigue of this component or others like the fastener system but allows the axle load from the train to spread over more sleepers/ties. In contrast, stiff pads cause larger dynamic actions on the infrastructure components such as sleeper and ballast material. Low stiffness rail pads of less than 100 kN/mm have been recommended in a number literature implying a potential neglect of associated problems of excessive rail displacement caused by very soft rail pads. This is the basis for motivation of this study to analyze the effects of rail pad stiffness on ballasted railway track so as to recommend rail pad stiffness that contributes towards minimal rail displacement and sleeper acceleration.

A 3D numerical model was established using ABAQUS/CAE 6.14 to carry out the investigation. The FEA model entails a rolling wheel, UIC 54 rail, rail pads, concrete sleepers, ballast and subgrade. The prepared model was verified with a laboratory experiment that replicated a ballasted track section (from one reference paper [1]). The basic parameters used in the model were synonymous to that of the experimental test and was in compliance with literature and the different standards such AS1085.14, AREMA and other acknowledged publications. Track behavior was noted in the form of stress, displacement, acceleration and corresponding rail seat loads to categorize the stiffness of the rail pad, that limits the negative extremes in track behavior. Parametric studies were executed with various rail pad stiffness to understand their consequence on the behavior of track components; rail and sleeper.

This study showed that, with increase in rail pad stiffness at 200 and 300 kN/mm rail pad stiffness, the rail vertical displacement decreases by at least 64-73% and 79-83%, rail vertical acceleration decreases by 37-56% and 56-77%, while rail vertical stress increased by 44-57% and 68-73%, the rail seat loads increased by 52-56% and 68-74% under static loading and increased by 37% and 55% under dynamic loading, the sleeper vertical acceleration increased by 55% and 62%. Due to correlation behavior of most of the out puts with increasing stiffness of rail pads, rail vertical displacement and sleeper vertical acceleration were chosen as the two criteria for selecting the most suitable rail pad stiffness.

Even though some researchers recommend soft rail pads below 100 kN/mm rail pad stiffness, which could increase rail movements and deflection, this research study has recommended rail pad stiffness of 150 kN/mm with 48% reduction in rail displacement and 44% increase in sleeper acceleration. This is also in an agreement with recommendation of Nazmul Hasan (2019) [2], that the softest rail pad should not be less than 100 kN/mm and desired range is 116-256 kN/mm.

Key Words: Modeling, Analysis, Ballasted track, Rail pad, Stiffness.

ACKNOWLEDGEMENTS

My upper most gratitude goes to the Almighty God who has graciously made it possible for me to conclude this thesis work through His blessings of good health throughout this study. I would like to direct my honest appreciation to all my instructors at African railway center of excellence for the kind of assistance they offered to me from the beginning of this graduate program. In precise, the guidance provided by my advisor, Henok Fikre (PhD) was crucial in producing this research work.

I would like to recognize the invaluable assistance and motivation provided by my entire family led by my wife Ms Cherop Esther and the contributions of all friends during my study. Finally, I wish to thank all those whose support was a landmark in the accomplishment of this study.

TABLE OF CONTENTS

LIST OF FIGURES

LIST OF TABLES

LIST OFABBREVIATIONS AND SYMBOLS

SDOF	Single Degree of freedom
BOEM	Beam on Elastic Foundation
FEA	Finite Element Analysis
FEM	Finite Element Methods
RSD	Rail seat deterioration
S	Sleeper spacing
$k_{railpad}$	Rail pad stiffness
k_{system}	Support system stiffness
$k_{sleeper:}$	Sleeper stiffness
EI:	Rail flexural rigidity (per rail)
UIC	International Union of Railways
HDPE:	High-density polyethylene
EVA:	Ethylene vinyl acetate
TPE	Thermoplastic polyester elastomer
MPa	Mega pascal
USP	Under sleeper pads
k	Stiffness or spring constant
U	Modulus of Elasticity
VSRP	Very stiff rail pad
SRP	Stiff rail pad
SORP	Soft rail pad
GUI	Graphical user interface
AREMA	American Railway Engineering and Maintenance of way Association
AREA	American Railroad Engineering Association
x_1	Length to zero deflection of the rail from point of maximum deflection
β	Fourth root of the ratio of track modulus and 4EI
EI	Rail flexural Rigidity
I	Second moment area of inertia
P	Wheel load
MUSP	Medium under-sleeper pad
SOUSP	Soft under-sleeper Pad
DEM	Discrete element modeling
μ	Coefficient of friction
RCF	Rail contact force
dBA	Sound power level
DIF	Dynamic Impact Factor

1. INTRODUCTION

1.1 Background

Public transport consists of extensive networks and a wide variety of transport services. As a strategy to tackle the growing demand for transport, service providers in the past tried expanding the existing networks and kept expanding them till they meet those demands [3]. Railway infrastructure**,** has become the most competitive transport means because of its unique advantages (efficiency, transportation capacity, low environmental impact, etc) and its contribution to reducing congestion on road networks [4]

One of the focal current worries in rail public transport is the risk of train operation associated with track degradation which lowers train safety and increases fatigue of track structure [5]. Although the degradation of rail tracks is usually slow, it may result high-risk failures with enormous financial maintenance costs [6]. Railway track which is too stiff can be the basis of load concentrations as the train load is spread over less supports and this in turn can result to amplified ballast attrition and generate disparities in track stiffness and thus differential settlement [7], [8]. Track which is not stiff enough, however, might lead to extreme rates of settlement and various types of subgrade related failure [7].

Figure 1. 1 Visual appearance of a deteriorated ballasted railway track [9]

Geometry degradation, as well as noise and vibration, have been recognized as problems that require to be reduced, which could be likely be achieved by amending track vertical stiffness and

finding a more homogeneous stiffness along the track [10]. One measure to mitigate these problems includes the use of elastic elements (e.g. rail pads, under-sleeper pads, and under-ballast mats) in the railway track [9].

Rail pads are typically made from polymeric compound materials is the regularly used resilient element, and is very crucial as it act as a softening medium between rail track and sleepers [11]. According Nazmul Hasan (2019) [2], rail pads play a significant part in track dynamics, influencing overall track stiffness, load distribution, and rail deflection. The rail pad has a load-distributing effect. In other words, when the track is loaded by the train, a soft rail pad permits a larger deflection which could lead to the fatigue of this component or others like the fastener system. Nonetheless, they lead to a more uniform distribution of stiffness throughout the railway system and the axle load from the train is spread over more ties [2] .

In contrast, stiff pads cause larger dynamic actions on the infrastructure components such as sleeper and ballast material. Though, on the positive side, they have a longer service life and decrease rail vibrations. Previous problems arising from improper or inadequate utilization of' rail pads include cracking of sleepers at rail seats, high settlements of tracks, and ballast/subgrade breaking from heavy damping. These problems result in lower load capacity and deficient structural adequacy of track substructures requiring costly maintenance and rehabilitation budget [12].

Even though, several studies have been done on investigating the effect of rail pad stiffness on vehicle-track dynamic properties [12]–[14], [15] including optimization of railway track stiffness [8], [16], [17], they focused much on rail pad stiffness effects on track behavior, by observing indicators such as noise radiation level, track component interactive forces (wheel-rail, rail-sleeper and sleeper-ballast) [11], rail displacement, ballast vibration and sleeper stressing among others. In a number of the literature reviewed, use of soft rail pads of an average 100 kN/mm or less has been recommended where the dominant rail pad stiffness range under the different studies were between 20 to 600 kN/mm [2], [10], [18], [19], [11].

Whereas rail pads of 100 kN/mm or less reduces on rail seat loads and sleeper acceleration, it neglects associated problems of soft rail pads such as excessive rail displacement, movement, vibrations and noise levels from wheel-rail contact as detailed in table 2.5. According to Chris A.

Murray (2014) [20], excessive rail displacements can result in reduced rail traffic speeds and heightened risk of derailments, with the potential for significant economic, environmental, and public safety impacts.

In view of the above background, this thesis study was carried out to suggest stiffness of rail pads that takes into account, both reducing rail displacement and sleeper acceleration to contribute towards mitigation of track structural degradation. Rail vertical displacement and sleeper vertical acceleration were attributed to have close link to drivers of degradation.

1.2 Statement of Problem

Throughout train operation, the vehicle-track interaction creates high impact loads and fatigue, which leads to degradation of railway infrastructure. This phenomenon is escalated by the demand for increased train speed and axle load resulting into excessive rail displacements, increased transmitted loads to the underlying track layers (sleepers, ballast and subgrade), track acceleration and vibration. To mitigate these effects, installing resilient materials is one of the strategy to inhibit high impact and destructive forces from train loading [8]. Among the resilient materials is the rail pad and reduces the load damaging effect through provision of flexibility to the track and acting to cushion the shocks and vibrations generated by the train wheel's movement [14]

A number of previous studies have been done on the influence of rail pad stiffness on the performance of ballasted railway track. The findings presented focused on modification of track support stiffness using rail pads as a resilient material to mitigate issues related to, track vibration levels, noise (sound power levels), displacement, rail seat loads, track component interaction forces and vehicle-track dynamic forces. Rail pads of low stiffness of an average of 100 kN/mm or less was predominantly recommended implying a potential neglect of associated problems of excessive rail displacement, movement, vibrations and noise levels caused by soft rail pads. This is the basis for motivation of this study.

Even though, the rail pads with lower stiffness causes excessive rail displacement and acceleration, the concentrated load reaching the sleeper top surface or rail seat area is less since the wheel load is spread over more sleepers. On the other hand, stiffer rail pads are beneficial in reducing rail displacements and acceleration, however it leads to increased concentrated loads at

the rail seat (RSL) and sleeper acceleration which causes damaging effect to the sleepers and consequently on underlying ballast and subgrade. Therefore, this study analyzed the rail pad stiffness effects on rail vertical displacement and sleeper vertical acceleration in a ballasted railway track and hence contribute towards reduced track degradation through recommending rail pad stiffness that takes care of the two extremes.

1.3 Research Objective

1.3.1 General objective

The general objective of this research was to model and analyze the stiffness of rail pads effects on ballasted railway track subjected to static and dynamic load so as to recommend rail pad stiffness that contributes to minimal rail displacements and sleeper acceleration.

1.3.2 Specific Objectives

The specific objectives of the research were;

- To analyze rail vertical displacement and stress under static loading with rail pad stiffness variation
- To evaluate the effects of rail pad stiffness on rail vertical acceleration, displacement and sleeper vertical acceleration under dynamic loading.
- To assess the influence of rail pad stiffness on rail seat loads for both static and dynamic loading
- To select a suitable rail pad stiffness based on rail displacement, and sleeper acceleration

1.4 Research Questions

The research questions which this thesis aimed to address included;

- What is the effect of varying rail pad stiffness on rail displacement, acceleration and stresses under static loading?
- How does the rail and sleeper vertical acceleration respond under dynamic loading with pad stiffness variation?
- How do the load concentrations (RSLs) change at the rail seat or sleeper top surface?

- What could be the most suitable rail pad stiffness that allows low rail displacement and sleeper acceleration?

1.5 Methodology

The existing literature on related topics from internet and reports, books, journals and other publications, research papers and sources available in electronic media were reviewed. The basic design parameters and input data were obtained from experimental test data that replicated a ballasted track section M. Sol-Sánchez (2016) [1] and from different foreign standards like AS1085.14, AREMA, Chinese Standard and other acknowledge publications.

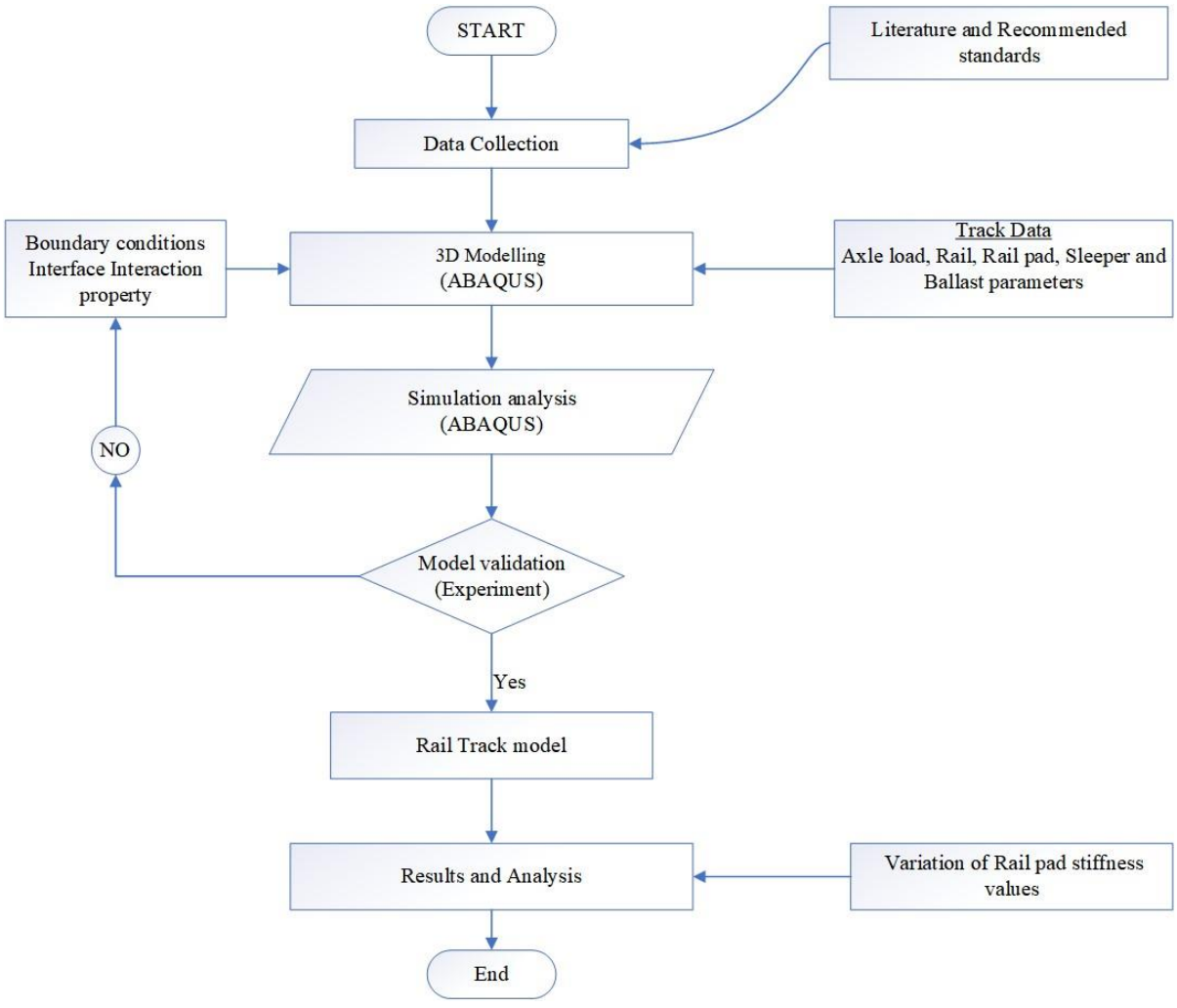

Figure 1. 2 Schematic layout of methodology

- Generally, the following was followed in this research; Input parameters were obtained from experimental test data and partly from recognized standards such as AREMA and other acknowledged publications.
- Three-dimensional ballasted railway track model in Abaqus/CAE commercial software package was prepared and validated with a laboratory experiment.
- Using the parameter values for validated track section model, a typical ballasted traction model was prepared for parametric studies and analysis.
- Static and dynamic analysis was conducted to study the behavior of the track (stresses and displacements, acceleration and rail seat loads). Dynamic analysis simulations were employed by conducting implicit analysis.

1.6 Significance of the Research

The output of this research will contribute to wider knowledge on the use of rail pads in minimizing ballasted track stress levels and impact loading. It can also serve as one of the reference materials for design and construction of flexible tracks to meet different operating conditions either as a standalone elastic element or else guiding decisions while considering combination of different elastic elements.

The output of this research work will be used by;

→ Different researchers,

→ Students and

→ Flexible ballasted track designers

1.7 Scope and Limitation

The research was focused on modeling and analysis of rail pad stiffness under static and dynamic loadings and studying the behavior of track parameters such as displacement, acceleration, stresses and rail seat loads. Simulations were conducted using Abaqus commercial software. Only, the vertical wheel load was considered, the other track loadings were not considered.

1.8 Organization of the thesis

This thesis is presented in 5 chapters as follows:

- Chapter 1 gives a brief background and the problem statement of the research. The objective, the scope, and the research methodology and limitations to the research are found in this chapter.
- Chapter 2 presents literature review on ballasted track components, track loading (static and dynamic), use of elastic elements in railway tracks, review of effects rail pad stiffness on track behavior, some numerical modelling using finite element packages of ballasted track also reported.
- Chapter 3 describes the research methodology that includes; material properties selection, finite element modelling methods and rail pad stiffness analysis
- Chapter 4 presents the results and discussion: this part contains the numerical analysis results with variation in rail pad stiffness.
- Chapter 5 Conclusion and recommendations. In the final chapter, the research thesis has been concluded and further research areas have been suggested.

2. LITERATURE REVIEW

2. 1 Track Structure

The performance of a railway track system results from a complex interaction of the system components in response to train loading. Both superstructure and substructure of railway tracks are equally significant in safeguarding the safety and comfort of passengers, quality of the ride and component life [21]. The typical shape and construction profiles of a ballasted track are illustrated in fig 2.1. The superstructure consisting of rails, fasteners and sleepers and the substructure consists of the ballast, subballast, and subgrade. The properties of the substructure components are much more variable and difficult to define than those of the superstructure [22].

The railway track structure has to accomplish two key functions: To guide the train directionally with safety and to carry and distribute the train load to the subgrade [23]. The track structure is required to; guide vehicles without risk of derailment, take up vehicle forces, off-load these forces via the track grid and ballast bed into the subsoil, ensure high passenger comfort and high availability for train traffic [22].

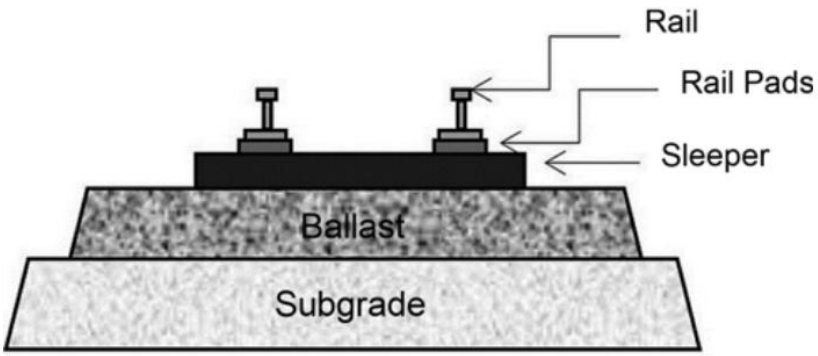

Figure 2. 1 Cross section of ballasted track structure [24]

Ballasted track is a type of traditional railway tracks. Ballasted track is commonly composed of steel rail, railroad tie/sleeper, railway fasteners and ballast bed [25]. Theoretically, ballasted track is the creation of railway track development. Generally, a layer of gravel is laid between ground and railway sleeper to form the track bed. Ballasted track a improve the flexibility and make track easy to repair [25].

The advantages of ballasted track are; ballasted track requires low investment cost, ballasted track is usually easy to lay, ballasted track has good drainage performance and high elasticity due to ballast. Some of the disadvantages of the ballasted track include; train run on the ballasted track with banged sound and low speed so that, passengers may feel uncomfortable, ballasted track is easy to be deformed, requires frequent and costly maintenance, train speed is limited and ballasted track has poor life expectation (about 15-20yrs).

2.1.1 Ballasted track structural components

Rails are longitudinal steel members that directly guide the train wheels evenly and continuously. They must have sufficient stiffness to serve as beams which transfer concentrated wheel loads to spaced sleeper supports without excessive deflection between the supports [26]. The profile of the rail surface together with wheel profile influences the guidance of the vehicles as they roll. Also, the rail and wheel surface defects can cause large dynamic loads which are detrimental to the track structure [22].

Sleepers are essentially beams that span across and tie together the two rails [25]. The key functions of sleepers are; to safely transfer loads from wheel axles to foundation [27], hold the fastening system to maintain proper track gauge, restrain the lateral, longitudinal and vertical rail movement by anchorage of the superstructure in the ballast [23]

Ballast is the main structural part of railroad where the sleepers or ties are laid. Its main functions is to transfer the loads coming from the super structure to the subgrade without failure and providing good drainage [28] and to provide stability to the track by withstanding vertical, longitudinal, and lateral forces [29]. Angular, crushed, hard stones and rocks uniformly graded, free of dust and dirt, and not prone to cementing action have been considered good ballast materials [22].

The layer between the ballast and subgrade is the subballast. It fulfills two functions which are also in the ballast list and these are; Reduce the traffic induced stress at the bottom of the ballast layer to a tolerable level for the top of the subgrade and extent the subgrade frost protection. The subballast reduces the otherwise required greater thickness of the more expensive ballast material. The most common and most suitable sub ballast materials are broadly-graded naturally

occurring or processed sand gravel mixtures, or broadly-graded natural crushed natural aggregates or slags [30].

The subgrade is the platform upon which the track structure is constructed. Its main function is to provide a stable foundation for the subballast and ballast layers [22]. The influence of traffic induced stresses extends downwards as much as five meters below the bottom of the sleepers. This deep layer must have sufficient bearing capacity, provide good drainage and yield a tolerably smooth settlement in order to prolong track serviceability [25]. Hence the subgrade is a very important substructure component which has a significant effect to track performance and maintenance [22].

2.1.2 Elastic elements

With the growth in rail freight traffic and demand for high train speeds, most railway infrastructure systems are being incorporated with elastic elements as standard practice [24]. These elastic elements alter the stiffness of the track and moderate phenomena such as ballast liquefaction, noise emission, and wave propagation [9]. This is due to the fact that, elastic components can be manufactured with different stiffness levels and high damping capacity. The polymeric nature of these elements means that they are lightweight, highly resistant, corrosion-proof, and easy to mould [9].

However, one of the foremost problems of elastic elements used in railroads is the deterioration triggered by environmental agents such as temperature, oxidation, or hydrolysis. For this reason, they have a useful life of approximately 20 years [31], [32]. However, the most frequently used devices are rail pads, under-sleeper pads, and under-ballast mats [9], which can distribute loads and reduce the noise emissions and vibrations stemming from the movement of rails, sleepers, and ballast, while mitigating the impact of these elements on each other.

2.1.3 Rail pads

Rail pads are a provision of comforting element between the steel rail and concrete surface. They transfer the rail load to the sleeper and filter out the high frequency force components [13], [33]. The rail pad stiffness should be as low as possible, the lower limit is determined by three factors:

increased wear and fatigue loading on other fastening components, increased dynamic gauge widening (rail roll) in curves and increased noise emission from the rail.

Rail pads are required between the rail seat and concrete sleeper surface [34] to fulfill the following functions; provide resilience for the rail/sleeper system, provide damping of the wheel induced vibrations, prevent or reduce rail/sleeper contact attrition and provide electrical insulation for track signal circuits [23], [35].

2.1.4 Rail pad types and classification

Rail pads are normally made out of rubber, high-density polyethylene (HDPE), thermoplastic polyester elastomer (TPE), and ethylene vinyl acetate (EVA) [36]. However, new elastic elements have been made from other materials, with emphasis upon those made from used tires [37]. As a general rule, these pads come in various designs in order to better adapt to the railway system, and can thus range in thickness from 4.5 to 15.0 mm. Rail pads are usually 180 mm long and 140 mm wide under rail type UIC 54, and 180 mm long and 148 mm wide under rail UIC 60. The use of this component improves load distribution, thus a smoother ride, and a better conservation of the superstructure.

Since contact surfaces between rail and sleepers are rigid, this elastic rubber is necessary as the stiffness of rail pads also plays an important role [11]. The rail pad stiffness affects the damping of the rail and the degree of coupling between the sleepers and the rail. In the case of very resilient rail pads the sleepers are well isolated from the rail vibration, but the vibration can propagate relatively freely along the rail. Equally, for stiff pads the rail vibration is limited by the coupling to the sleepers and damping of the pads but the sleeper vibration is greater.

European standards categorize rail pads as follows [2]; soft rail pads have a stiffness of less than 80 kN/mm, medium rail pads have a stiffness between 80 and 150 kN/mm, and hard rail pads have a stiffness of 150 kN/mm or more. Rail pads for heavy-haul freight or industrial lines fall under the hard type, and rail pads for conventional, high-speed, and transit lines may fall under any type (soft, medium, or hard) in European classification [2].

The classifications of rail pads (soft, medium, and hard) are relative to track stiffness. In other words, a pad classified as hard for a particular track may qualify as soft for another track.

Classification is based on balancing the increasing effect of rail pad stiffness on the characteristic length of track against the decreasing effect of rail pad stiffness on P_2 load and is presented in table 2.1

Table 2.1 Classification of rail pad stiffness in relation with the track stiffness [2]

Track stiffness (kN/mm)	Rail pad stiffness (kN/mm)				
	Very soft	Soft	Medium	Hard	Stiff
50	112–125	>125–150	>150–200	>200–250	>250
60	135–150	>150–180	>180–240	>240–300	>300
70	157–175	>175–210	>210–280	>280–350	>350
80	180–200	>200–240	>240–320	>320–400	>400

The rail pad stiffness variation of 0 to 5000 MN/m values cover the range of all modern rail pads [36], from very soft rubber, to polymeric, to high-density-polyethylene, or EVA pads as in table 2.2

Table 2.2 Dynamic stiffness of commercial railway pads [36]

Type	Stiffness (MN/m)	Visual identification
Rubber	20–100	Soft
Studded polymer	200–800	Soft
Polyurethane	800–1200	Medium
High density polyethylene (HDPE)	800–2500	Hard
EVA	3000–3500	Hard
Steel	5000+	Very stiff

Classification of rail pad stiffness keep varying depending on standards and consulted bibliography [9]. The stiffness of rail pads mostly in use varies roughly from 50 to 250 kN/mm. The stiffness of a conventional ballasted track is usually in the range 50–60 kN/mm, and that of a high-speed track is in the range 70–80 kN/mm. A rail pad contributes 34%, and ballast and subgrade together contribute 65% toward the total elastic behavior of a concrete tie track [2]

2.2 Review on articles related to the research topic

I. Grossoni et al (2016) [38] considering low travelling speed (40 km/h) and medium support stiffness (100 MN/m) found that, it is possible to minimize the ballast pressure which is associated with track settlement, the excessive contact patch energy (linked with wear and RCF) and the rail-pad forces (linked with component fatigue) with the softest pads, while the stresses

on the rail head and foot (linked with component fatigue) with the stiffest pads. It has been demonstrated how it is possible to drastically improve the crossing performances finding the optimum value of pad stiffness, in some cases reaching 20% reduction. The maximum achievable reductions that were achieved vary from 5% to 20%. Each speed and each type of support has different requirements and, therefore, it is not possible to find a unique solution. As general rule, if the line type is slow, it is possible to use soft/medium pads, while if the speed increases it is better to use medium pads. The study considered ballast degradation resulting from ballast pressure changes as a key indicator of track degradation.

According to Konstantinos Giannakos (2011) [39], the rail pad stiffness affects the damping of the rail and the degree of coupling between the sleepers and the rail. In the case of very resilient rail pads, the sleepers are well isolated from the rail vibration, but the vibration can propagate relatively freely along the rail and for stiff rail pads, rail and sleeper coupling is increased and thus sleeper acceleration. It is therefore crucial to consider the effects on both rail displacement and sleeper acceleration when choosing rail pad stiffness to mitigate track stressing or loading conditions on the different components which was the essence of this study.

C. Wan et al (2016) [40] carried out a study on Optimization of the elastic track properties of turnout crossings specifically by using combination of rail pads and under sleeper pads found that, the softer rail pads can significantly reduce the dynamic forces acting on the crossing nose, application of stiffer USPs can slightly reduce the high-frequency force (P_1) but increase the low-frequency forces acting on the sleepers and the ballast bed, less-stiff USPs with higher damping can reduce the low-frequency forces caused by the low frequency component of the wheel force, the bending moments in the rails, rail displacements and deformation of rail pads are decisive for the choice of the optimum properties.

Kedia, Naveen Kumar et al (2021) [24] reported that, since it is impractical to change all the components and properties of a track structure, only equivalent stiffness and damping of the track structure is varied by using soft to stiff pads. Rail pad stiffness values in the range of 100 to 600 kN/mm were used in the study. The track modification was performed by varying rail pads and the observation was that; stiffer pads reduced velocity level between 7 dB to 24 dB and noise level between 8 dBA to 14 dBA. Thus, this paper recommended Indian ballasted track structure for use of stiffer pads. whereas this study reports general reduction in track velocity and

noise levels, this is attributed to reduction in rail displacement and acceleration since increasing rail pad stiffness at the same time increases track noise due to increased sleeper vibrations or acceleration.

J.I. Egana et al (2006) [18] substituted the conventional rail pads by softer pads on a test curve and found that soft pads reduce corrugation growth and eliminate one of the wavelengths developed when using stiff pads. Furthermore, the test shows that, a stiffness of 60×10^6 N/m was sufficient to eliminate the corrugation wavelength.

Jabbar Ali Zakeri et al (2020) [19], carried out a study on the effect of pad stiffness on rail displacement with different support sleeper conditions. The model was investigated using different pad stiffness (0.6 to 2.4×10^8 N/m). Fig 2.2 presents the rail displacement related to each pad stiffness. As it can be seen, the vertical displacement of the rail is reduced by increasing the pad stiffness.

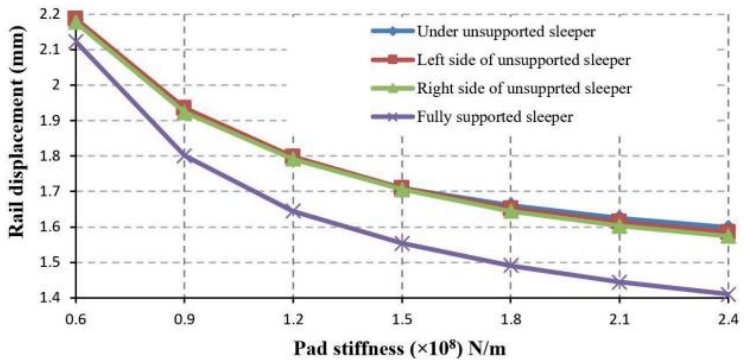

Figure 2. 2 Rail vertical displacement in various pad stiffness [24]

This study emphasized on reduction in rail vertical displacement with increasing rail pad stiffness without any comment on the effects caused on sleeper vertical acceleration and increased rail seat loads.

Jabbar Ali Zakeri et al (2008) [11] showed that, by increasing rail pad stiffness from 50 MN/m to 250 MN/m, interaction forces of ballast-sleepers and sleeper-rails increase by about 9%. Increase of rail pad stiffness, from 50 MN/m to 250 MN/m, caused a decrease of 45% in displacement of the rail

Patrícia Ferreira et al (2018) [8] conducted experimental measurements and computational estimations consisting of work that describes a track optimization procedure developed to select

combinations of rail pads and USPs to be installed in a reference railway track in order to improve its dynamic response to high-speed trains circulating at speeds ranging from 300 to 400 Km/h. The most commonly used resilient material however is the rail pad and whereas combination with USPs results in better outcome, it is as well increases on the costs.

Leposava Puzavac et al (2012) [41], presented that, in order to avoid quick deterioration of the ballast material and thus track geometry deterioration, maximum vibration speed in the ballast should not exceed 15 to 18 mm/s. From this study as shown in fig 2.3, for the speeds of 250 km/h the measured vibrations are almost 30 mm/s. Also, it is shown that using pads of stiffness 20 to 60 kN/mm can decrease the speed of vibrations in the ballast.

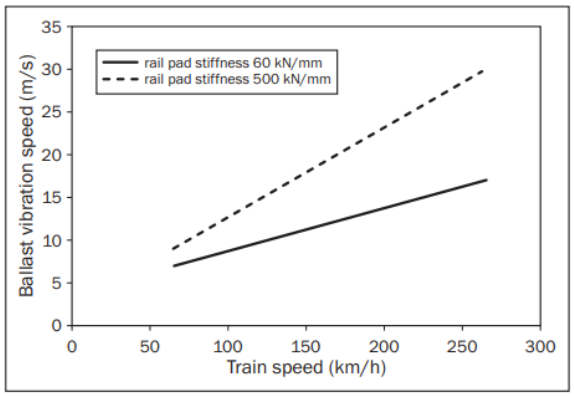

Figure 2. 3 Influence of rail pad stiffness on vibrations in the ballast

It was observed that, low rail pad stiffness of 60 kN/mm keeps ballast acceleration at acceptable levels and little is mentioned about the extent of rail displacement which as well impacts the safe track operation such as increase fatigue of the component and resistance to forward train movement.

2.2.1 Effect of Rail pad stiffness on ballasted track stiffness

According Nazmul Hasan (2019) [2], rail pads play an important role in track dynamics, influencing overall track stiffness, load distribution, and rail deflection. The relations between track parameters (e.g., between the track stiffness and the track modulus and between the characteristic length and the track modulus) in the following two established formulas taken from the relevant literature are used to evaluate the effect of reduction in track stiffness by rail pad on the track modulus and the characteristic length:

$$k = \frac{1}{4}\sqrt[3]{\frac{K^4}{EI}} \qquad \text{eq 2.1}$$

where k = track modulus (N/mm/mm or lb/in/in)

K = track stiffness (N/mm or lb/in)

and EI = bending stiffness of rail (N/mm^2 or lb/in ^{2})

$$L = \sqrt[4]{\frac{4EI}{K}} \qquad \text{eq 2.2}$$

where L = characteristic length (mm or in).

The effect of reduced track stiffness on the track modulus and the characteristic length is presented in table 2.3. A rail pad with a stiffness of 1,300 kN/mm would reduce track stiffness by 4%, which corresponds to a reduction in track modulus by 5.3% and an increase in characteristic length by 1.4% (given in table 2.3, row for p of 4%). Thus, very stiff pads would have little effect on the track modulus and the characteristic length (i.e., load distribution) and therefore also on ballast pressure. It is of little use to use a very stiff pad that does not increase the characteristic length appreciably.

Table 2.3 Effect of reduction in track stiffness, ρ, on the track modulus, k, and the characteristic length, L Nazmul Hasan (2019) [2]

p (%)	n	Reference: K (kN/mm)	ρ (kN/mm)	k reduces by (%)	L increases by (%)
1	101	50	5,050	1.3	0.3
2	51	50	2,550	2.7	0.7
3	34	50	1,717	4.0	1.0
4	26	50	1,300	5.3	1.4
5	21	50	1,050	6.6	1.7
10	11	50	550	13.1	3.6
15	7.7	50	383	19.5	5.6
17	6.9	50	344	22.0	6.4
20	6.0	50	300	25.7	7.7
25	5.0	50	250	31.9	10
30	4.3	50	217	37.8	12.6
35	3.9	50	193	43.7	15.4
45	3.2	50	161	54.9	22.1
50	3.0	50	150	60.3	26.0
55	2.8	50	141	65.5	30.5
60	2.7	50	133	70.5	35.7
65	2.5	50	127	75.3	41.9
70	2.4	50	121	79.9	49.4
75	2.33	50	117	84.3	58.7
80	2.25	50	113	88.3	71.0
81	2.23	50	112	89.1	74
88	2.14	50	107	94.1	102.7

An increase of over 10% characteristic length is assumed to be the minimum requirement and corresponds to a 30% reduction in track stiffness. For a very stiff track, the maximum characteristic length is 0.7 m. By contrast, 1.2 m is a typical characteristic length in a ballasted track.

A rail pad with a stiffness of 107 kN/mm would reduce track stiffness by 88%, which corresponds to a reduction in track modulus of 94% and an increase in characteristic length of 102.7% (from 0.7 to 1.4 m) (table 2.3, row for p of 88%). This would be unacceptable, as a characteristic length of 1.4 m is poor, and rail stress would increase by 100%. Furthermore, softer rail pads lead to increased lateral tilting of the rail. Thus, a reduction in track stiffness of 30%–80% induced by rail pad is acceptable.

The classifications of rail pads (soft, medium, and hard) are relative to track stiffness. In other words, a pad classified as hard for a particular track may qualify as soft for another track. Classification is based on balancing the increasing effect of rail pad stiffness on the characteristic length of track against the decreasing effect of rail pad stiffness on P_2 load [2]. Considering a conventional track stiffness range of 50–100 kN/mm, the stiffness range of rail pad is 112–300 kN/mm, are recommended and the recommended desirable stiffness is in the range of 116–256 kN/mm [2]

2.2.2 Suitability of soft and stiff rail pads

With respect to general track behavior, it is known that the use of softer rail pads produced larger rail deflection, which could lead to the fatigue of this component or others such as the fastener system. Nonetheless, they lead to a more even distribution of stiffness throughout the railway system. In contrast, it was found that stiff pads cause greater dynamic actions on the infrastructure and ballast material. However, on the more positive side, they have a longer service life and reduce rail vibrations. Thus, from the experiences and studies recorded by Miguel Sol-Sánchez (2014) [9], table 2.4 shows a scheme of the optimal field of application of the rail pads according to their vertical static stiffness.

Table 2.4 Field of application of rail pads according to its stiffness Miguel Sol-Sánchez (2014) [9]

Field of application	Stiff pads	Soft pads
Reduction of damage in sleepers		✓
Decrease in the stress transmitted to sublayers		✓
Impact attenuation		✓
Reduction in corrugation		✓
Decrease in rail deflection. Lower energy consumption	✓	
Reduction in stiffness changes		✓
Lower rail movements. Longer life of fastener system	✓	
Reduction in rail vibrations	✓	
Lower level of noise from wheel–rail contact	✓	
Reduction in sleeper and ballast vibration		✓

2.2.3 Effect of rail pad stiffness on track noise

When the pad stiffness is increased, the sleeper is coupled to the rail over a large range of frequency and its component of the sound dominates [42]. On the other hand, the rail vibration especially in the vertical direction experiences greater damping due to this coupling to the sleeper and its noise radiation is reduced. For softer rail pads, the opposite effects are seen [42], [9]. The dependence of each of the noise components of the rail pad stiffness is illustrated in the fig 2.4.

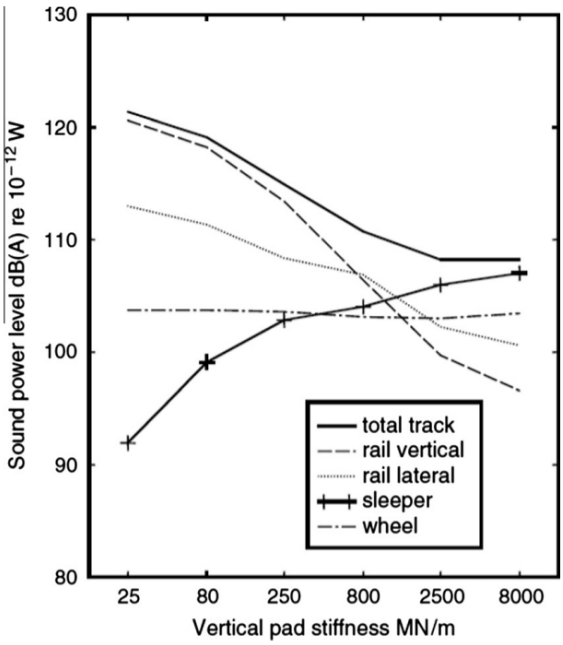

Figure 2. 4 Influence of pad stiffness on noise generation [42], [9]

2.3 Track components and loading

The purpose of the railway track structure is to provide safe and economical train transportation. This requires to serve as stable guideway with appropriate vertical and horizontal alignment. To achieve this role, each component of the system must perform its specific functions satisfactorily in response to the traffic loads and environmental factors imposed on the system. Thus, the superstructure and the substructure are separated by the sleeper ballast interface.

2.3.1 Static and Quasi-Static (Dynamic Ride) Loading

Static loading represents the mean weight of rail freight wagons, unchanged over a reasonably long period of time. The wheel/rail contact force would be identical to static wheel load when the ideal conditions of perfect wheel tread and rail surface are found [43]

Quasi-static loading slightly changes its magnitude over a long period of time. It is the sum of the static load and the effect of vehicle speed, together with track support and geometry (curvature, superelevation, and roughness) [43]

In contrast, **Dynamic loading** is time dependent. Its magnitude changes rapidly within the short period of time, which is dependent on the type of abnormalities [43]

2.3.2 Rail support stiffness or track spring rate (K/D)

Vertical track stiffness is a function of the modulus of elasticity of different layers and components in the railway track system. There are a number of methods which can be used to represent track stiffness mathematically, depending on different factors such as isolating the stiffness of some components, frequency excitations and track stiffness non-linearity [44]. Track Stiffness in the time domain, track stiffness (k) is generally defined as the ratio of track load F(t) and track deflection d(t) in the linear part of the rising phase of the load [10].

$$K = F(t)/ d(t) \qquad \text{eq 2.3}$$

In the stiffness analysis;

- Rail is assumed to be a beam on an elastic foundation
- Modulus of Track Elasticity, u (or k) (Track Modulus)

Comprehensive support stiffness is the force acting on the top surface of the rail support, to make the rail support top surface produce one unit deflection, is the comprehensive of the support stiffness under the rail as demonstrated in fig 2.5.

$$\frac{1}{D} = \frac{1}{D_f} + \frac{1}{D_s} + \frac{1}{D_b} \qquad \text{eq 2.4}$$

The eq. 2.2 is for calculating track stiffness is a serial connection. Track modulus (u) is obtained by dividing the track stiffness by sleeper spacing;

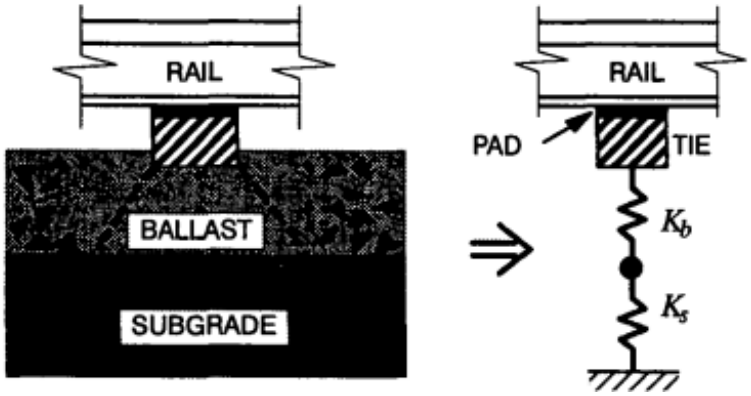

Figure 2. 5 Support stiffness under the rail [45]

$$u = \frac{D}{a} \qquad \text{eq 2.5}$$

where a is sleeper spacing

The stiffness on concrete sleeper is very big and can be taken as infinity (∞)

The definition of composite or global track system stiffness $S_{composite}$ is the point load required to produce a unit deflection of the rail at the location where the load is applied. K_{system} arises from the railpad modulus $K_{railpad}$ and the trackbed modulus $K_{trackbed}$ acting in combination. These are related by the well-known formula for springs in series

$$\frac{1}{k_{system}} = \frac{1}{k_{rail\,pad}} + \frac{1}{k_{sleeper}} + \frac{1}{k_{ballast}} \qquad \text{eq 2.6}$$

For a quasi-static analysis, it does not matter that the trackbed and the rail pad are separated physically by the rigid sleeper. [46]

Table 2.5 Spring rates (stiffness) of individual rail track components, LUBER (1961) [44]

Component	**Soft wood sleeper (kN/mm)**	**Hard wood sleeper (kN/mm)**	**Steel sleeper (kN/mm)**	**Concrete sleeper (kN/mm)**
Sleeper	50 - 150	300 - 500	2000 -4000	8000 - 20000
Ballast	50 - 300	50 - 300	50 - 300	50 - 300
Overall spring rate (without ballast and formation)	30 - 110	40 - 290	50 - 310	50 - 430
Overall spring Rate	20 - 80	20 - 130	20 - 170	30 - 180

2.4 Rail pad Dynamics

The traditional ballasted track consists of rail tracks, pads, and sleepers laid on ballast and subgrade. In this system, rail pads usually made from polymeric compound materials" are mounted on rail seats and tend to attenuate the dynamic stress from axle loads and wheel impact from both regular and irregular train movements. These pads are crucial as they act as a softening medium between rail track and sleepers [9]. Previous problems arising from improper or inadequate utilization of' pads include cracking of sleepers at rail seats, high track settlements at global and local levels, and ballast/subgrade breaking from heavy damping. These problems result in lower load capacity and deficient structural adequacy of track substructures requiring costly maintenance and rehabilitation budget. The rail pads therefore has been of interest to the rail engineers as they reduce dynamic stresses and impact loads on sleepers [12]

Rail pads can be arranged as elastic and dashpot components of a simple mass-spring-damper. The spring can be assumed to be linear, and the damping is assumed to be proportional to the deformation rate of the rail pad. According to the comparison between track models and measurements, it’s important to include the rail pads to get an accurate track model. The stiffness of the fastening is normally much less than that of the rail pad. Therefore, when investing track dynamics, the role of the fastenings is normally neglected

2.5 Track Modelling

For structural analysis of the track, a number of computer packages are available. Especially programs based on finite element method can perform very detailed analysis of displacements, stresses and strains of track components. However such a modelling of a track structure requires

a vast amount of elements, especially under loading condition corresponding to a moving train or under other conditions causing wave propagation [17], [30], [47]. Overtime many researchers have used several approaches to come up with suitable model railway track and vehicle. The kind and extent of the model is dependent on the results required.

2.5.1 Rail as a Beam on Elastic Foundation (BOEF)

Continuously supported models of infinite length are based on the beam on elastic foundation theory. The rail, pads, fastenings, sleepers, ballast, sub-ballast and subgrade are components that define the value of the modulus of track elasticity. In a historic view, the BOEF model is by far the Classic Method and also forms the backbone of many subsequent improvements made to track design as in fig 2.6

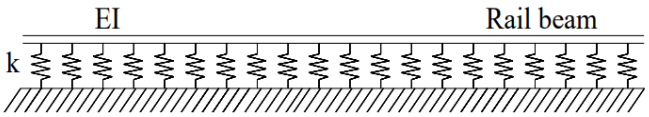

Figure 2. 6 Beam (Bending stiffness) on elastic foundation (Bed modulus) [27]

The composition of this track model is: the rail is represented by a simple (Euler) beam with mass and bending stiffness, resting on a uniform linear spring to represent the ballast. The sleeper masses are distributed uniformly and added to the rail density to give the beam density. The model has a sound mathematical formulation with quite clear simple physical interpretation.

It assumes the rail modeled as an infinite Euler-Bernoulli beam with a continuous longitudinal support from a Winkler foundation, which may be regarded as equivalent to an infinite longitudinal line of vertical, uncoupled and elastic springs. The distributed force supporting the beam then is proportional to the beam deflection. By only using two track parameters the rail deflection w(x) could be obtained from the differential equation [30], [48], [46]

The concept of a foundation modulus to represent the rail support was first introduced by Winkler (1867), when he analyzed the rail as an infinite beam supported on a continuous linear elastic foundation.

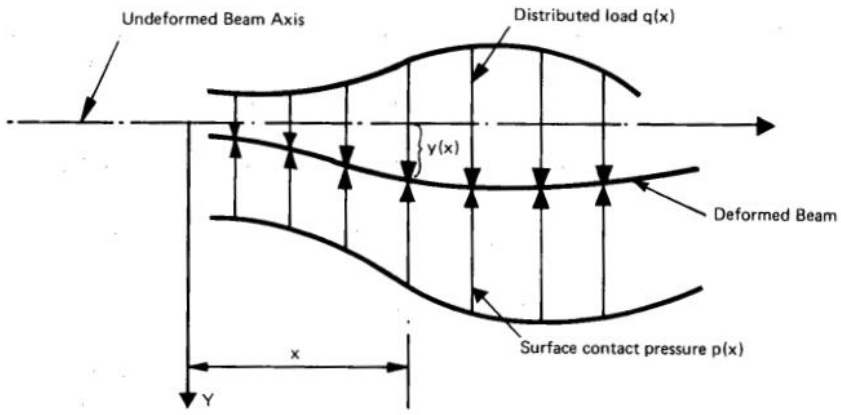

Figure 2. 7 Equilibrium position of a deformed beam subjected to load q (X) [44]

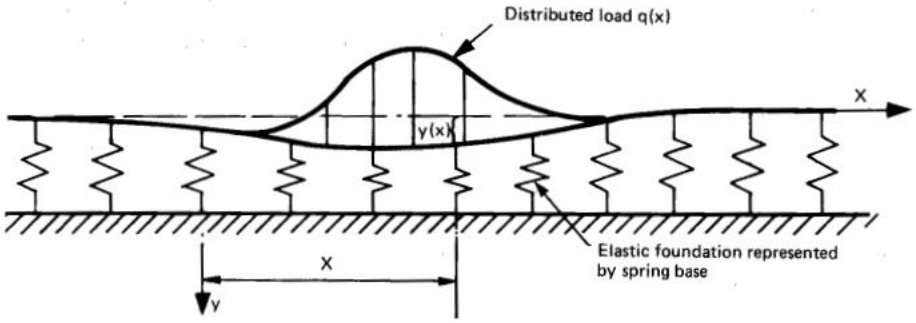

Figure 2. 8 Representation of a continuously supported infinite beam on an elastic foundation subjected to load q (X) [44], [49]

$$EI\frac{d^4y}{dx^4} + p(x) = q(x) \qquad \text{eq 2.7}$$

Where;

y(x) = vertical deflection at X,

q(x) = distributed vertical load,

EI = flexural rigidity of the rail,

p(x) = continuous contact pressure between the sleeper and ballast,

p(x) = ky(x), and k = modulus of the foundation.

Hence the Winkler equation becomes;

$$EI\frac{d^4y}{dx^4} + ky(x) = q(x) \qquad \text{eq 2.8}$$

This equation may be represented as the response of an infinite beam attached to a spring base, subjected to a load q(x), fig 2.6. The general solution of the Winkler equation has been developed in detail by Hetenyi (1946). Since the rail is subjected to wheel loads, which are concentrated loads, the relevant solution to Winkler's equation must be restated in terms of the design wheel load, P, instead of load q(x). The solution of the rail deflection, rail shear force and rail bending moment at any position X, (X positive), from the load point are [50], [51] :

- Rail deflection

$$Y_x = \frac{P\beta e^{-\beta X}}{2K}(\cos\beta X + sin\beta X) \qquad \text{eq 2.9}$$

- Rail shear force,

$$V_x = \frac{Pe^{-\beta X}}{2}\cos\beta X \qquad \text{eq 2.10}$$

- Rail bending moment

$$M_x = \frac{Pe^{-\beta X}}{4\beta}(\cos\beta x - sin\beta X) \qquad \text{eq 2.11}$$

Here β includes the flexural rigidity of the beam as well as the elasticity of the supporting medium, and is an important factor influencing the shape of the elastic beam. For this reason, the factor β is called the characteristic of the system, and, since its dimension is $(\text{length})^{-1}$, the term 1/β is frequently referred to as the characteristic length. Consequently, the product βX will be a dimensionless number with

$$\beta = \left(\frac{u}{4EI_Z}\right)^{0.25} \qquad \text{eq 2.12}$$

where k = track modulus (MPa)

E = Young's modulus of the rail steel (MPa), and

I = rail moment of inertia (mm^4).

The Winkler equation was originally developed for longitudinally sleepered track, and has since been applied to transversely sleepered track, thereby raising questions concerning the validity of the assumption of continuous rail support. But although there have been many methods developed to analyze track on the basis of discrete elastic supports, according to Ken (1976) the results obtained are not significantly different from those using the Winkler model [44]. Hence

considering the rail as a beam on a continuous linear elastic foundation is generally regarded as the most acceptable method for the analysis of rail stresses and deflections [44].

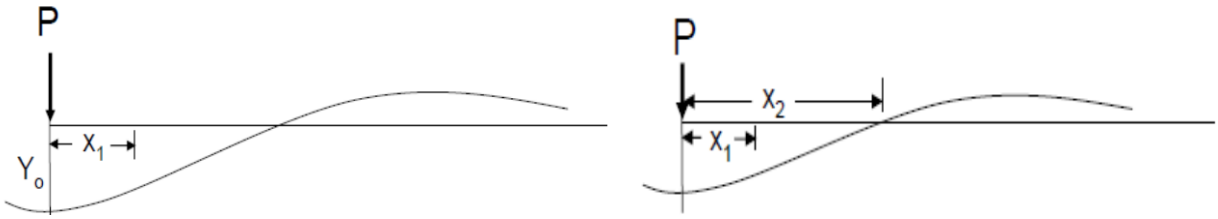

Figure 2. 9 Load deflection curve for the rail [48]

The distance x_1 (m) (Figure above) is that distance to the position of zero rail bending moment from the point of load application and is given by [48];

$$x_1 = \frac{\pi}{4}\frac{1}{\beta}$$

$$x_1 = = \frac{\pi}{4}\left(\frac{4EI}{u}\right)^{0.25} \quad \text{eq 2.13}$$

An Early Method for the Determination of k or u approach is promoted by the research of Timoshenko and Langer (1932), by use of loading device that consists of one axle. The rail deflection at the wheel, w_m, caused by wheel load P, is recorded and then collocated (i.e. equated) with the corresponding analytical expression obtained from eq. 2.9 at x=0; namely, by setting $w_m = w(0)$ [49].

The resulting equation is

$$w_m = \frac{P\beta}{2K} = \frac{P\sqrt[4]{\frac{K}{4EI}}}{2K} \quad \text{eq 2.14}$$

Solving it for Track modulus k, the only unknown, yields

$$K = \frac{1}{4}\sqrt[3]{\frac{P^4}{EIW_m^4}} \quad \text{eq 2.15}$$

Determination of Rail Seat Forces (Q or F)

Rail Seat Load: $Q_O = 0.391PS/x_1$ eq 2.16

Where:

P = Wheel Load

u or k = Track Modulus

S = Tie spacing

EI = Flexural rigidity of rail

E = Modulus of Elasticity of Rail

I = Rail Moment of Inertia

Similarly;

Rail Moment: $M_o = 0.318Px_1$ eq 2.17

Deflection: $Y_o = 0.391P/ux_1$ eq 2.18

NB: x_1 and u is obtained from eq. 2.13 and eq. 2.15 respectively

This model may be acceptable only for static loading of a track on soft support, for example a track with wood sleeper. Several evident limitations are inherent in the BOEF model. Such as the fundamental problem of circular definition when measuring k, which is not very helpful for the predictability; the assumption of continuous foundation and the response of the track is linear; materials behavior only in the vertical direction; shear deformation in the rails is not included; continuously welded rail are assumed ; not time dependent [30].

Several criticisms can be made of the realism of the BOEF model include; the sleeper mass is not distributed correctly, there is no provision for a rail pad to (partially) and sleeper bending effects are not considered.

2.5.2 Beam (rail) on discrete supports

In this model the supports could either be discrete spring-damper systems or spring-mass spring systems, modeling rail pads, sleepers and ballast bed.

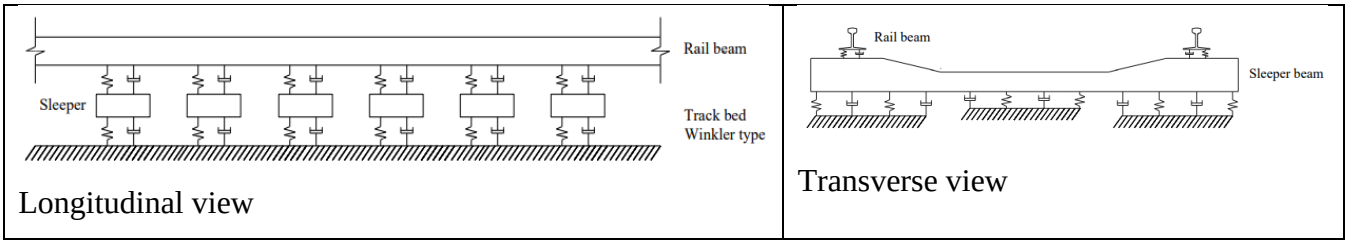

Figure 2. 10 Rail on discrete support

In a three-dimensional model, the rail (a beam element) is placed on a spring and damper in parallel. This spring-damper system models the rail pad. Below this another beam element,

modeling the sleeper, is placed. The sleeper rests on an elastic foundation, i.e., another spring – damper system, as in fig 2.10.

2.6 Weighted sum method for selection of rail pad stiffness

Many solution algorithms intend to combine all the multi-objective functions into one scalar objective using weighted sum

$$F(x) = \alpha_1 f_1(x) + \alpha_2 f_2(x) + \ldots\ldots + \alpha_P f_P(x) \quad \text{eq 2.19}$$

The important issue arises in assigning the weighting coefficients $\alpha_1, \alpha_2, \alpha p, \ldots\ldots$, because the solution strongly depends on the chosen weighting coefficients having a sum of 1

In this thesis, two objective functions; sleeper vertical acceleration (associated to track safety) and rail vertical displacement (associated with cost) are given as $f_1(x)$ and $f_2(x)$ respectively. Combining the two, the following scalar objective is given as:

$$F(x) = \alpha_1 f_1(x) + \alpha_2 f_2(x) \quad \text{eq 2. 20}$$

Where, α_1 and α_2 are the weighting coefficients with $\alpha_1 + \alpha_2 = 1$, α_1 and α_2 is from literatures.

Railway design have to consider safety over the whole project from development to maintenance. This is because, the safe by design principles actively eliminate risk during design development and maintenance activities [61]. This therefore implies that the safety should have a percentage greater than 50%. According to Jonan Backman in 2002 [52], in his study; a rail safety of 59% was reported with 41 % cost.

Table 2.6 Summary of Literature related to the topic

S/N	Author /Objective	Methodology	Findings
01	**Author** Miguel Sol-Sánchez et al (2014) [9] **Objective** To study the characteristics of elastic elements as well as the research carried out to	A state of the art review	-Experience led to the use of rail pads that were more resilient with stiffness values of less than 60–100 kN/mm - Replacing stiff rail pads (250 kN/mm with 40 kN/mm) reduced stresses transmitted to

	test and evaluate their effectiveness		the sleeper by up to 20% (in a ballasted track - Soft rail pads of 68.8 kN/mm stiffness increase the movements and vibrations
02	**Author** Jabbar Ali Zakeri (2008) [11] **Objective** To carry out sensitivity analysis of train-track dynamic interaction with variation in some parameters	DATI computer software was designed to simulate the vertical dynamic interactions between railway tracks and vehicles.	-Increasing rail pad stiffness from 50 MN/m to 250 MN/m, interaction forces of ballast-sleepers and sleeper-rails increase by about 9% -Increase of rail pad stiffness, from 50 MN/m to 250 MN/m, will cause a decrease of 45% in displacement of the rail
03	**Author** Xiaolin Song et al (2020) [13] **Objective** To investigate possible solutions to the excess train–track dynamic interaction excited by rail corrugation	Numerical analysis was performed based on a vehicle–track coupled dynamical model with field-measured rail corrugation information	New rail pads with a stiffness of 35 MN/m, which are softer than the original rail pads with a stiffness of 50 MN/ m, were recommended in the study.
04	**Author** Jabbar Ali Zakeri1et al (2020) [19] **Objective** The effect of axle load and pad stiffness on rail vertical displacement were investigated	Applying mathematical model and solving the equations via numerical integration in the time domain	By increasing the pad stiffness rail displacement decreased from 2 to 13 % in the unsupported sleeper and from 1 to 6 % in the partially supported sleeper.

05	**Author** Konstantinos Giannakos (2010) [39] **Objective** To investigate influence of the rail pad stiffness on the Railway track stressing and its life-cycle	An innovative methodology was proposed, verified in practice and used for the calculation of the loads acting on concrete sleepers.	The adoption of very soft pads reduced the track's stressing and led to a significant prolongation of the Life Cycle of the track elements.
06	**Author** Nazmul Hasan (2019) [2] **Objective** To design rail pad stiffness in terms of a general desirability range and to suggest a classification system	Analytical Study: Rail Pad Stiffness and Classification	The softest pad is defined to correspond to a 55% reduction in P_2 load and an 80% reduction in track stiffness. Thus, the stiffness of a rail pad should not be less than 100 kN/mm.
07	**Author** Naveen Kumar Kedia et al (2021) [24] **Objective** The paper focuses on the effect of short and long wavelength track irregularities and rail pads on train induced vibration and noise	A train-track interaction model where rail vehicle was modelled as a spring-mass-damper system, and a ballasted track structure was modelled as an infinite rail resting on the viscoelastic foundation.	The stiffer pads reduced velocity level between 7 dB to 24 dB and noise level between 8 dBA to 14 dBA. Also, the use of a stiff pad keeps the vibration and noise level within the permissible limits for both long and short-wavelength track irregularities. Rail pad stiffness study range (100-600) kN/mm
08	**Author** Sakdirat Kaewunruen (2008) [53] **Objective**	Laboratory approach; A high-capacity drop-weight impact testing machine was	The uses of rail pad clearly demonstrate the prevention of excessive dynamic stress from the rail to the railway sleepers

	To carry out experimental investigations, in order to evaluate the attenuation effect of rail pads on the impact behavior of railway concrete sleepers.	constructed at the University of Wollongong, Australia.	and can reduce up to 50% of dynamic bending moments at rail seat of the prestressed concrete sleepers.
09	**Author** Leposava Puzavac et al (1970) [10] **Objective** This paper analyses the track stiffness from the aspect of its influence on the quality of the vertical track geometry.	Numerical analysis	With the increase of the train speed, vibrations play a decisive role in the process of track geometry deterioration. It is shown that using pads of stiffness 20 to 60 kN/mm can decrease the speed of vibrations in the ballast
10	**Author** Amin Khajehdezfuly (2019) [54] **Objective** To investigate the effect of rail pad stiffness on the wheel/ rail force in a slab track with harmonic irregularity.	A two-dimensional numerical model was developed (Finite element analysis method). Rail pads stiffness used in the study were 20, 80, 150, 300, and 500 MN/m.	when the rail pad stiffness is increased, the DIF is increased (when the rail pad stiffness is varied from 20 to 500 MN/m, the critical speed is changed from 100 to 200 km/h and DIF is increased about 45%.).
11	**Author** Patrícia Ferreira et al (2019) [8] **Objective** To select combinations of rail pads and under sleeper pads which improves the dynamic response of the reference	Use of numerical simulations and real scale laboratory test	Results show that selected combinations of rail pads and under sleeper pads lead to reductions of around 30% in peak vertical ballast acceleration moving at speeds of 300 to 400 Km/h.

	railway track		
12	**Author** J.I. Egana et al (2006) [18] **Objective** To examine the influence of new rail pads on corrugation	Finite element analysis simulation and field measurements.	This result shows that, a stiffness of 60×10^6 N/m is sufficient to eliminate corrugation wavelength.
13	**Author** Xin Zhao (2018) [55] **Objective** To study the influences of the fastening stiffness, speed, and axle load on the dynamic vertical forces excited by contact surface unevenness for a heavy haul ballasted railway track.	The explicit FE modeling Note: The main component of the fastening system stiffness is rail pad stiffness.	-The DAF of the wheel–rail force first decreases with the fastening stiffness and then remains approximately constant after a critical value of 200–300 MN/m -The optimum fastening stiffness should be 150–200 MN/m.

3.0 METHODOLOGY

The methodology employed in this thesis brings together various fields that have been discussed previously in the literature review to answer the research questions. Broadly, the methodology section of this thesis employs the following research procedures:

- Evaluating the best fitting software
- Data Collection
- Finite element modeling
- Selection of Rail pad stiffness

3.1 Evaluating the best fitting software

The different finite element software was assessed to come up with the best fitting software for the modeling and analysis involved in this study as described as follows.

ANSYS: is user friendly environment, can uniquely simulate electromagnetic performance across component, circuit and system design, and can evaluate temperature, vibration and other critical mechanical effects. It requires heavy computational power to give accurate results for complex analysis and faster database is a requirement. Most suitable in energy industry, problems involving dynamics, statics, fluids, electromagnetic, thermal, and vibrations [56].

LS DYNA: ideal for dynamic analysis, capable of simulating complex real-world problems, handles large deformations, can simulate automotive crash and explosions. However, the graphical user interface is not interesting compared to other FE software, not efficient at implicit time integration. It is most applicable in automobile, aerospace, construction, military, manufacturing, and bioengineering industries [57].

PLAXIS 3D: primarily used for geotechnical analysis and simple geometric problems, staged-construction modeling and analysis capability is better, dynamics for load modeling and plax flow for groundwater analysis [58]. On the other hand, it requires heavy computational power and it is more expensive, Limited online tutorials available. It is application is centered on geotechnical analysis and rock mechanics.

NASTRAN [43]: used to analyze linear and nonlinear stress, dynamics, and heat transfer characteristics of structures and mechanical components. It has complex GUI, it is not a complete package, thermal resistance calculation is absent, not capable of performing acoustic analysis [59]. It is a general-purpose software.

ABAQUS /CAE, or "Complete ABAQUS Environment" which is a computer code application used for modeling and analysis of parts and assemblies (pre-processing) and visualizing the finite part analysis results [60]. ABAQUS has a wide variety of material models such as elastomeric and hyperelastic material modeling. The main Advantages using ABAQUS are:

Non-Linear Performance: Even though, FEA models do take time to run. The strength of the ABAQUS code that was originally developed as a nonlinear solver is that it will run any nonlinear simulation quicker and can converge on more true, additional realistic results than different codes.

Contact Modeling: Real applications square measure made from assemblies, not single components. The components of those assemblies operate by returning into contact with one another. ABAQUS is out and away the most effective FEA code at handling all styles of contact. Also, its CAE interface currently makes it elegantly straight forward for a typical user to line up several contacts within the FEM.

Efficient Substructures: ABAQUS supports standard substructure processes like super elements. The ABAQUS sub model method is elegantly straightforward enough. Fixing a functioning sub model from a world model is mostly performed in minutes. In recent years, the ABAQUS sub modeling capability was developed to operate with nonlinear analysis.

Extreme Deformation: ABAQUS package has been well matched for nearly thirty years to manage extreme deformation simulations [15] because of its intrinsic nonlinear code.

Fracture and Failure: ABAQUS offers a general framework for modeling bulk material damage and failure over a large variety of materials (composites, metals, concrete, etc.) and structures. This framework permits simulation of damage initiation and evolution while not the necessity for specifying any initial state within the structure.

Development and Support: ABAQUS user community contributes documented examples using ABAQUS for unique applications. On top of this, the presence of this documentation, amounting to thousands of articles and papers [61] makes it preferable by designers.

The issue with ABAQUS is that the 3D modeling features are not advanced to accommodate complex shapes. Because of this, a 3D CAD design software, SOLIDWORKS is parallelly used in modeling.

Consequently, looking at the above merits this software embraces and observing successful researches done by means of this software in adding to the fact that many tutorials on this specific field of study exist better than the other FE software, ABAQUS was chosen to be used in this study.

3.2 Modules for model formulation

Most models created in Abaqus/CAE are assembled from different parts. It always starts with creating different parts separately in the parts module. Different parts may need different material properties, which are defined in the property module. A full range of material properties are available in ABAQUS, such as elastic and plastic behavior, as well as thermal and acoustic behavior. The model then is assembled in the assembly model, by combing the different instances originates from different parts. In the step module the analysis is divided [60], [47]

3.3 Element formulation

An element's formulation refers to the mathematical theory used to define the element's behavior. In the absence of adaptive meshing all of the stress/displacement elements in Abaqus are based on the Lagrangian or material description of behavior: the material associated with an element remains associated with the element throughout the analysis, and material cannot flow across element boundaries. In the alternative Eulerian or spatial description, elements are fixed in space as the material flows through them [47]

Abaqus has an extensive element library to provide a powerful set of tools for solving many different problems. All elements used in ABAQUS are divided into different categories, depending on the modeling space. The element shapes available are beam elements, shell

elements and solid elements and the modeling space is divided into 3D space, 2D planar space and axisymmetric space [60].

3.3.1 Solid Element

Among the different element families, continuum or solid elements can be used to model the widest variety of components. Conceptually, continuum elements simply model small blocks of material in a component. Since they may be connected to other elements on any of their faces, continuum elements, like bricks in a building or tiles in a mosaic, can be used to build models of nearly any shape, subjected to nearly any loading.

Solid elements in two and three dimensions are available in ABAQUS. The two-dimensional solid element allows modeling of plane and axisymmetric problems. In three dimensions the isoparametric hexahedron element is the most common, but in some cases complex geometry may require tetrahedron elements. Those elements are generally only recommended to fill in awkward parts of mesh.

3.3.2 Spring and Dashpot elements

Spring and dashpot elements are widely used. For instance, the rail pads between the rail and the sleeper, connectors for bounding adjacent ballasts in each direction, and the boundary conditions for constraining the sleepers. SPRING1 and SPRING2 elements are available only in Abaqus/Standard. SPRING1 is between a node and ground, acting in a fixed direction. SPRING2 is between two points with its line of action being the line joining the two nodes, so that this line of action can rotate in large-displacement analysis. The spring behavior can be linear or nonlinear in any of the spring elements in Abaqus. The spring and dashpot have longitudinal or torsional capability in one, two, or three-dimensional applications.

The longitudinal spring-damper option is a uniaxial tension-compression element with up to three degrees of freedom at each node: translations in the nodal x, y, and z directions. No bending or torsion is considered. The torsional spring-damper option is a purely rotational element with three degrees of freedom at each node: rotations about the nodal x, y, and z axes. No bending or axial loads are considered. The spring-damper element has no mass. Masses can

be added by using the appropriate mass element, the spring or the damping capability may be removed from the element.

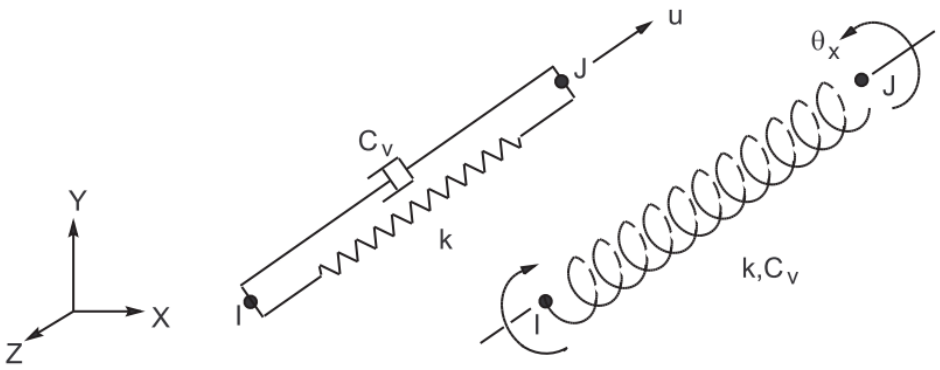

Figure 3. 1 Spring and Damper [62]

3.4 Data collection

The primary input data for the numerical validation model, which replicated the actual ballasted track section was obtained from a reference laboratory experiment explained as follows;

M. Sol-Sánchez et al (2016) [1] with the aim of evaluating the effect of using different configurations for the railway track conducted a laboratory experiment, in order to replicate the various track sections that can be applied in railway infrastructures. The box used in the study, whose appearance is shown in fig 3.2 a, was 440 mm in width, 750 mm in length, and 500 mm in height, allowing for the simulation of the railway track section under the rail seat area (with a sleeper spacing near 500 mm), where the highest levels of stress over ballast are expected. The testing box includes a piece of a concrete sleeper (250 mm in width and 357 mm in length), whilst the rail used was a type UIC-54EI with a length of 250 m.

A subgrade layer composed of 2 cm of compacted sand over the metallic floor of the box, presenting an elastic modulus of approximately 70 MPa in fig 3.2 b and fig 3.2 c also shows the control of the density of the granular layers used in this study (by means of a Pavement Quality Indicator device, PQI) in order to guarantee its appropriate compaction [63].

In preparation of track model using the track properties in table 3.1, efforts were made to ensure that, the track component materials (Rail, Rail pad, Sleeper, Ballast and Subgrade properties

were equal or closed to that of the physical experiment in the laboratory. The different missing parameters were obtained from published ballasted track model analyses researches

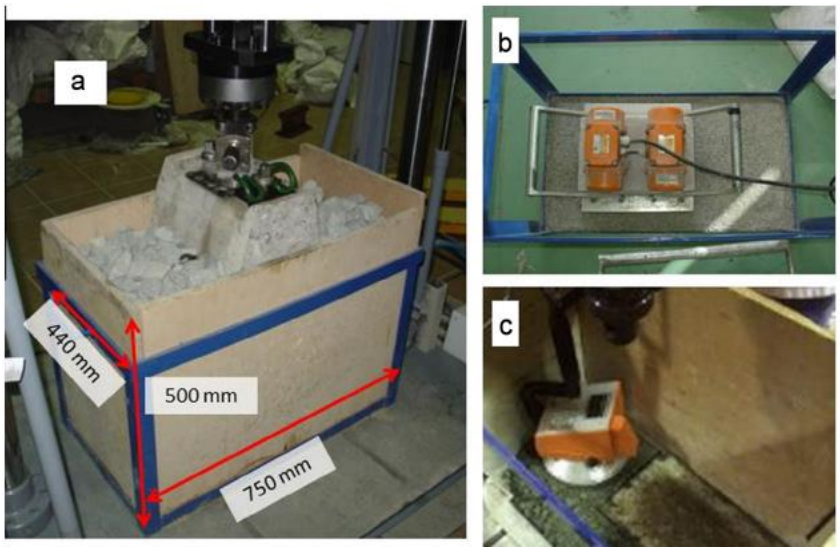

Figure 3. 2 Visual aspect of (a) the box used for the study, (b) the compaction of a sandy layer to simulate the subgrade, (c) and a control of the compaction of granular layers [1]

3.4.1 Input data for validation model

Most of these data were obtained from the laboratory reference experiment and the missing data was obtained from relevant standards and literature.

Track properties used for Abaqus Validation model

Table 3.1 Track properties used for Abaqus Validation model

Material property	**Track components**					
	Rail	**Sleeper**	**Ballast**	**Subgrade**	**VSRP**	**SRP**
Young's modulus, E (MPa)	210000	35000	150	70	700	210
Poisson's ratio,ν	0.28	0.2	0.3	0.25	0.42	0.4
Unit weight, γ (Kg/m^3)	7850	2400	3240	1600	950	811
Spacing (mm)	1500	500	N/A	N/A	500	500

The rail, sleeper, rail pad and the geomaterials comprising the track substructure (ballast and subgrade) are all modelled with solid C3D8R elements assumed to be linear elastic. The different parts of the ballast section were modeled in Abaqus and assembled as in the fig 3.3. The international rail profile UIC54 has been used for the simulation in compliance with the physical laboratory model. The width of the sleeper of 250 mm was used as in the laboratory experiment and the depth of 200 mm was adopted [64].

.

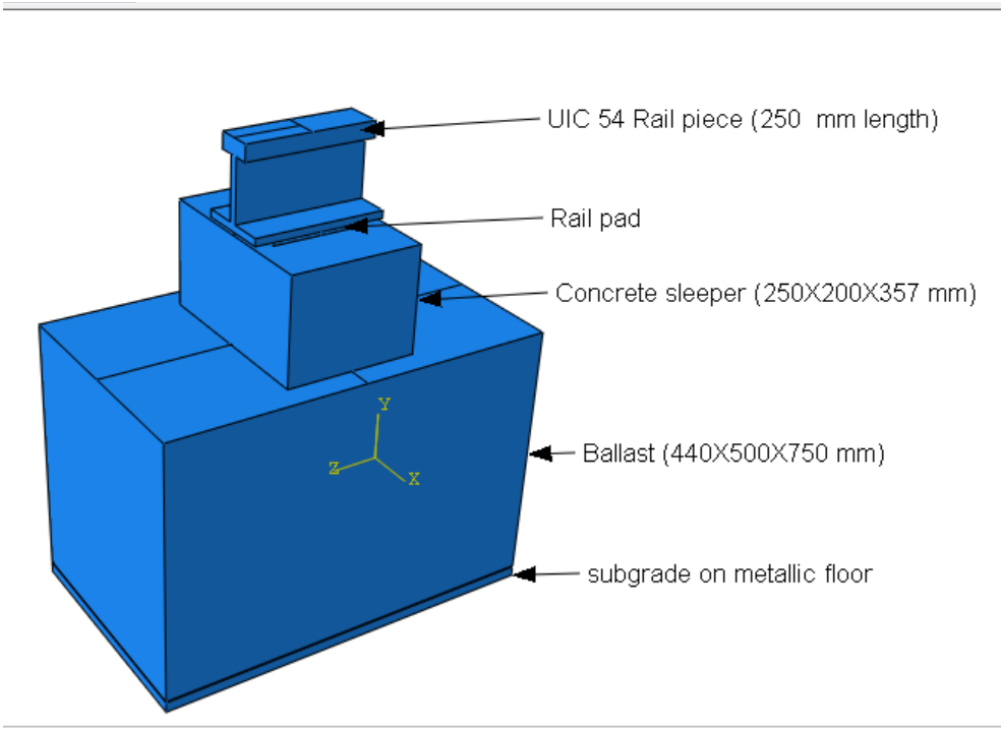

Figure 3. 3 Abaqus ballasted track validation model

The input parameters for the rail pads were obtained from a list of tabulated material properties for a variety of engineering materials such as metal, ceramic, composite and polymers by Massachusetts Institute of Technology [65]. The young's modulus and density of the VSRP made of Polyethylene (HDPE) was read as 700 MPa and 950 Kg/m^3 respectively. The young's modulus of the SRP was interpolated using stiffness relationship between VSRP and SRP, the density of SRP was obtained to be 811 Kg/m^3. The poisons ratio was read as 0.42 and 0.40 for Polyethylene and Deconstructed tire tread layers respectively.

3.4.2 Force-displacement curves for experimental and numerical comparison

Force-displacement curves were obtained by applying forces; 5, 10, 15, 20 and 25 kN force for the two cases (when using VSRP and SRP between rail and sleeper).

The boundary conditions selected for the model was of type “axisymmetric” and are detailed as follows

- At the bottom of the model, all the translations and rotations were fixed ie encastre (U1 = U2 = U3 = UR1 =UR2 =UR3 = 0). This was to simulate the metallic floor supporting the structural components in the experimental setup and simulates under lying structures in actual environment.
- At the sides, the translations normal to the vertical planes were fixed ie in the longitudinal direction, fixing z displacement (U3 = UR1 = UR2 = 0) and in the lateral direction, fixing x displacements (U1 = UR2 = UR3 = 0). The justification was to simulate the continuity of the track at boundary regions.

Fig 3.4 shows the force displacement curves for the experiment having different configurations of elastic elements ie rail pads (VSRP, SRP and SORP), combinations (VSRP and MUSP, VSRP and SOUSP) [1]. However, for the purposes of model validation, only force- displacement curves for very stiff rail pad (VSRP) and stiff rail pad (SRP) were considered.

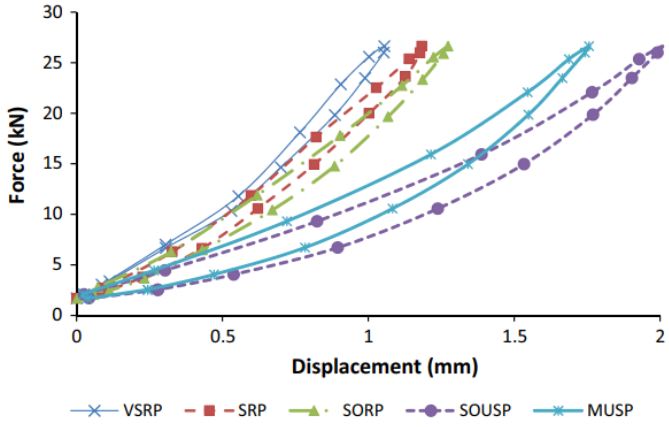

Figure 3. 4 Force-displacement curves measured for the configurations with different elastic elements over ballast layer [1].

The corresponding displacement values of the different forces for the experiment were extracted from fig 3.4 and tabulated together with numerical force-displacement results in table 3.2 for VSRP and SRP respectively.

Table 3.2 Force-Displacement Results for both experimental test and numerical simulation

Force (kN)	Displacement (mm)			
	VSRP		SRP	
	Experiment	Numerical	Experiment	Numerical
5	0.2073	0.1674	0.1958	0.1897
10	0.4756	0.4515	0.3915	0.4566
15	0.6951	0.6273	0.5873	0.7458
20	0.8780	0.8131	0.7831	1.0261
25	1.0244	0.9688	0.9788	1.0579

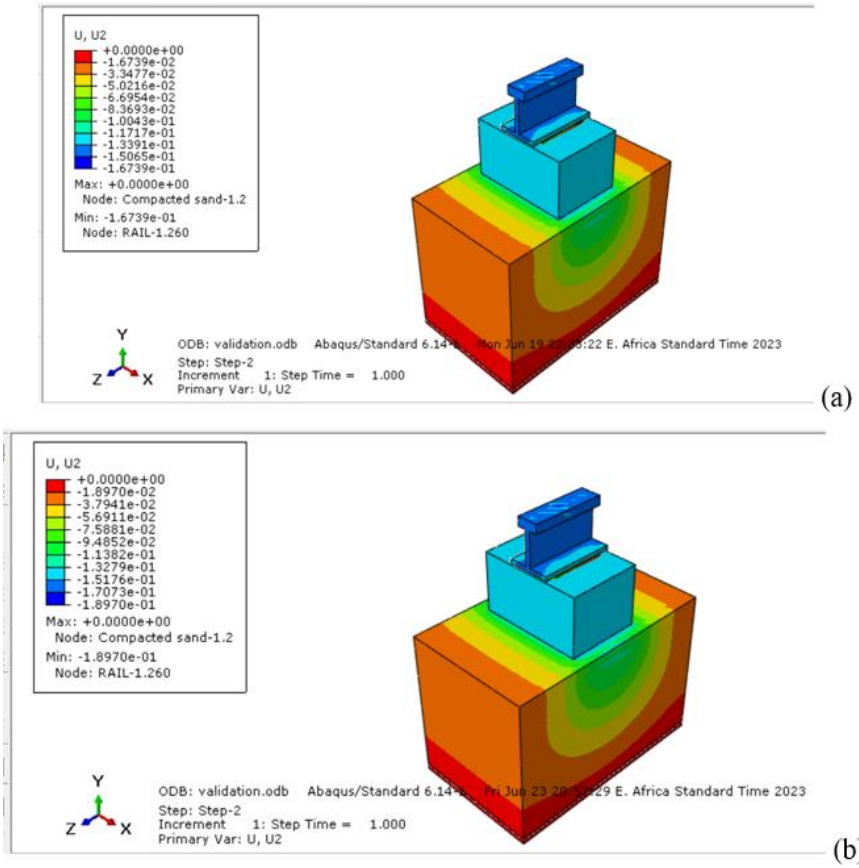

Figure 3. 5 Showing vertical displacement for the model with VSRP (a) and with SRP (b) at 5 kN loading

The results in the table 3.2 were then illustrated graphically for both numerical and experimental test with reference to very stiff rail pad and stiff rail pad (VSRP and SRP) in the figures 3.6 and 3.7

Force-Displacement curve for VSRP, Experimental and Numerical

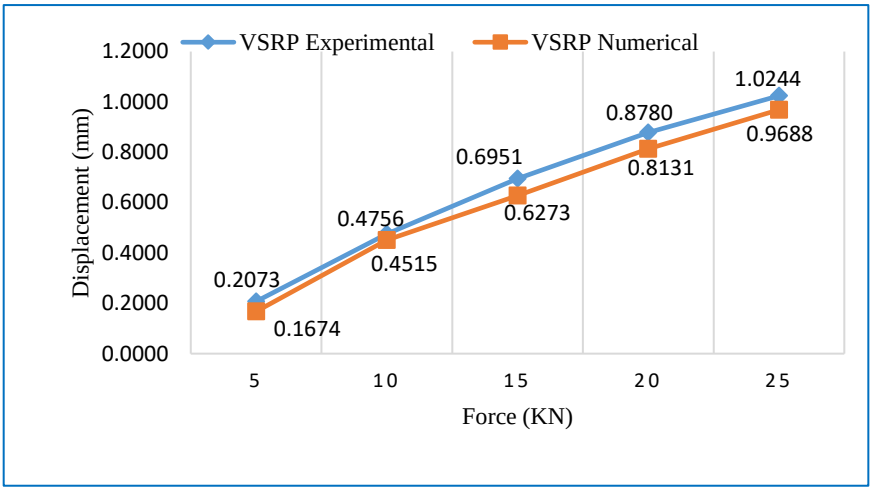

Figure 3. 6 Force-displacement curve for both Numerical and Experimental using VSRP

Force-Displacement curve for SRP Experimental and Numerical

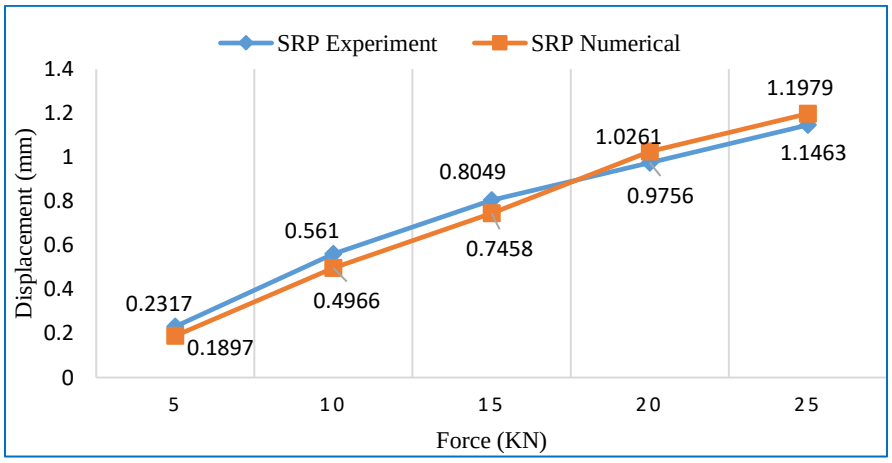

Figure 3. 7 Force-displacement curve for both Numerical and Experimental using SRP

The force-displacement curves for both experiment and numerical results under the two case scenarios of VSRP and SRP correlate quite well proving that, the quality of FE model is good. The small deviations in the force-displacement curves between experimental and numerical analysis can be attributed to the following;

- The boundary effects applied in the model which may not replicate the exact representation of the experiment conditions
- The ballast young's modulus was not given and selecting one from literature and standards creates possibilities of deviations from the actual value possible in the laboratory environment.

Once the validation model was in fair agreement with respect to the experimental results, a ballasted railway track model was prepared using the same material properties.

3.5 Finite element ballasted railway track model preparation

Since the problem is symmetric, half of the track structure is simulated. The rail (UIC 54 kg/m) 159 mm high was modelled with solid elements (C3D8R). The rail rests on discrete rail pads, which have been modelled as a spring element (SPRINGA), with rail pad stiffness being the main parameter varied for the study. The concrete Monoblock sleeper dimensions 2.5 m x 0.25 m x 0.2 m (length x width x height) and spaced at 0.60 m. The substructure comprises the ballast and subgrade. The total simulated thickness is 1.809 m. Due to symmetry, only half of the problem geometry was considered, with the boundary conditions properly applied along the symmetry plane.

The length of the track considered was limited to 5 sleeper bays, arising from model size sensitivity analysis and considering the computational effort required to solve the 3D problem in the time domain. The vertical boundaries of the track structure are restrained against horizontal movement normal to each face [66], and a restraint is applied on all the three directions (X Y and Z) at the bottom face. The rail, sleepers and the geomaterials comprising the track substructure were all modelled with solid C3D8R elements assumed to be linear elastic.

3.5.1 Ballasted track model component's material properties

The component description, dimension, and material type of the track components used in the simulation are as described in table 3.3.

Table 3.3 Showing Material properties

Component description	Dimension	Parameter	Value	Unit

Rail	UIC 54EI 2.5 m length	Young's Modulus (E) Poison's ratio (v) Density (r)	210000 0.28 7850	MPa Kg/m^3

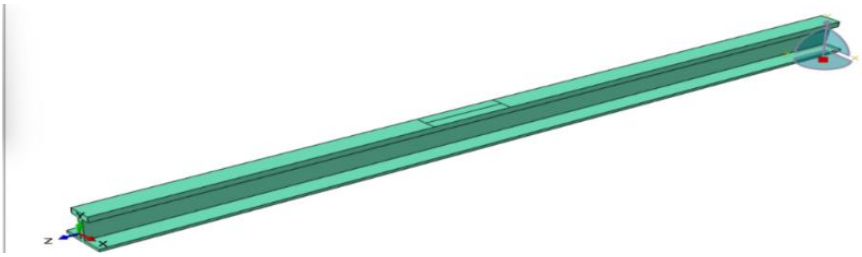

(a)

Sleeper	0.250 m width 0.200 m depth 1.250 m length	Young's Modulus (E) Poison's ratio (v) Density (ρ)	35000 0.2 2400	MPa Kg/m^3

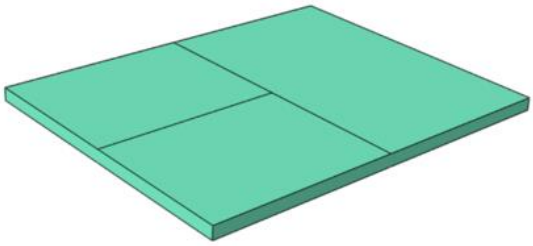

(b)

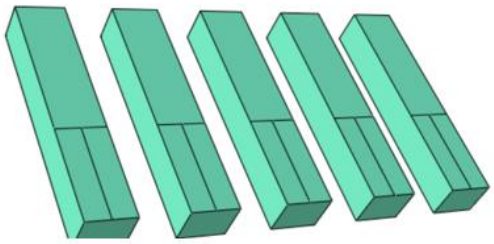

(e)

Component description	Dimension	Parameter	Value	Unit
Ballast	0.45 m depth 3.1 m width 2.5 m length	Young's Modulus (E) Poison's ratio (v) Density (ρ)	150 0.3 3240	MPa kg/m^3

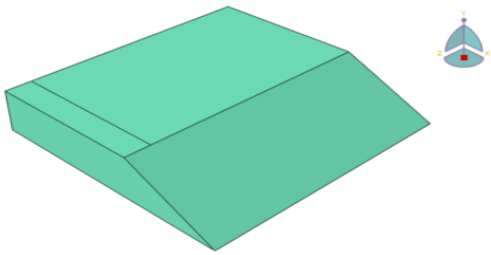

(c)

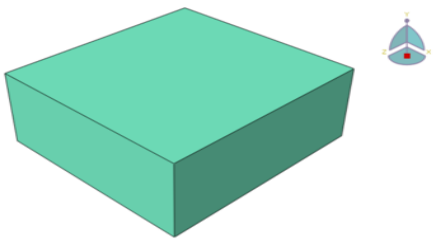

(d)

Figure 3. 8 (a) Rail (b) Rail pad (c) Ballast (d) Subgrade (e) Sleepers

Subgrade	1.00 m depth 2.350 width 2.5 m length	Young's Modulus (E) Poison's ratio (v) Density (ρ)	70 0.25 1600	MPa kg/m^3
Rail pad (VSRP/SRP)	1.00 m depth 2.350 width	Young's Modulus (E) Poison's ratio (v) Density (ρ)	700/210 0.42/0.4 950/811	MPa kg/m^3

[30], [1], [67], [68], [69]

Due to the fact that it's difficult to assign sketch profile to beam element in ABAQUS, approximated I-shape rail profile has been used. Compared to the actual rail profile the deviation of the approximated I-shape area moment of inertia value was less than 0.2%, which is negligible. Accordingly, the actual area moment of inertia (I_{xx}) for UIC 54EI rail is 2127 cm^4 and the calculated area moment of inertia for the adopted I-section of the rail profile is 2130 cm^4 giving a percentage difference of 0.14%.

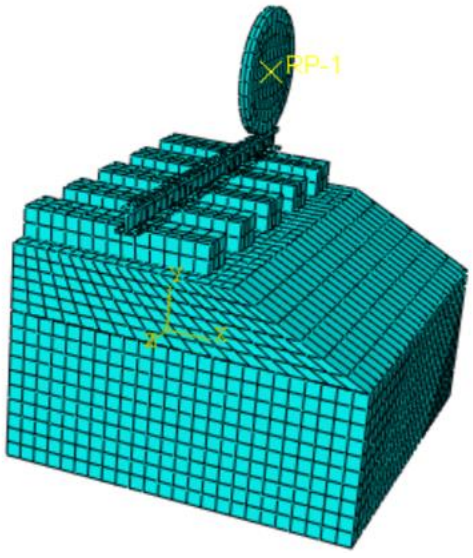

Figure 3. 9 Meshed assembly model for dynamic analysis

The additional material properties of the ballasted track model during dynamic analysis is the steel wheel which is modelled to simulate a moving load. The wheel part as indicated in the

track model assembly in fig 3.9 was considered to have the same properties as the steel rail material with a diameter of 920 mm [41].

3.5.2 Model size sensitivity analysis

Due to uncertainties in use of boundary conditions, different track model sizes produce different results considering a particular parameter. Generally, as the model size increases, so the quality of results however, this increases the required resource and computational time. For this thesis, the track model distances ranging from 3 sleepers to 9 sleepers were varied as in table 3.4 and corresponding track settlement results were obtained.

Table 3.4 Different track length settlement results

Track Distance (Length) (mm)	Number of sleepers	Settlement (mm)	Percentage decline in settlement with reference to 1.5 m length of track
1500	3	8.1346E-04	
2500	5	5.3304E-04	35%
3500	7	5.3362E-04	34%
4500	9	5.3400E-04	34%

The fig 3.10 shows typical track models at different distances or length of track. The results for model size sensitivity analysis shows a high decline in track settlement from size 1.5 m length of track to size 2.5 m length of track by 35%. For the next 3.5 m and 4.5 m length of the track, there was no perceptible further decline in settlement as the result converges or becomes asymptotic to imaginary straight line. Basing on these results and in consideration of computer computational time, 2.5 m length of track consisting of five sleepers was chosen.

Model size sensitivity analysis

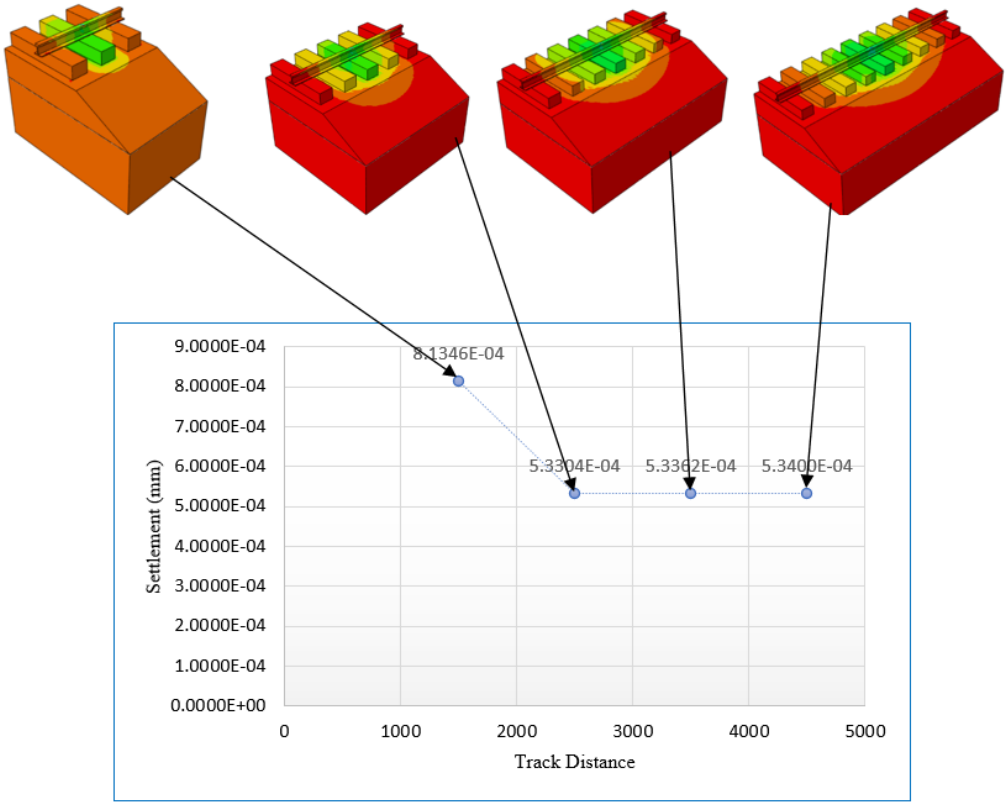

Figure 3. 10 Track model size sensitivity analysis

3.5.3 Element type and mesh sensitivity analysis

In the FE model, all the track components were meshed with C3D8R type of element which is an 8-noded linear brick, reduced integration element. The aim of mesh sensitivity analysis was to obtain optimum mesh size to be used in parametric studies. A point load of 125 kN was applied at the center of the track on the top of the rail. The displacement values were recorded with refinement in element size and the displacement was seen to converge at element size of 50 mm

The finer mesh takes almost 4752 seconds to compute compared to the coarser one that takes only 6.4 seconds. Thus, to maximize the computing time efficiency, a maximum mesh size of 50 mm × 50 mm is chosen for this study. The total number of nodes and elements in the simulation model was 70,050.

Table 3.5 Sensitivity analysis for mesh size selection

Element size (mm)	Deformation, E22	Computational time (seconds)
100x100	8.3086E-04	6.4
80x80	1.1231E-03	79
60x60	1.6856E-03	684
50x50	1.7385E-03	2854
30x30	1.7634E-03	4752

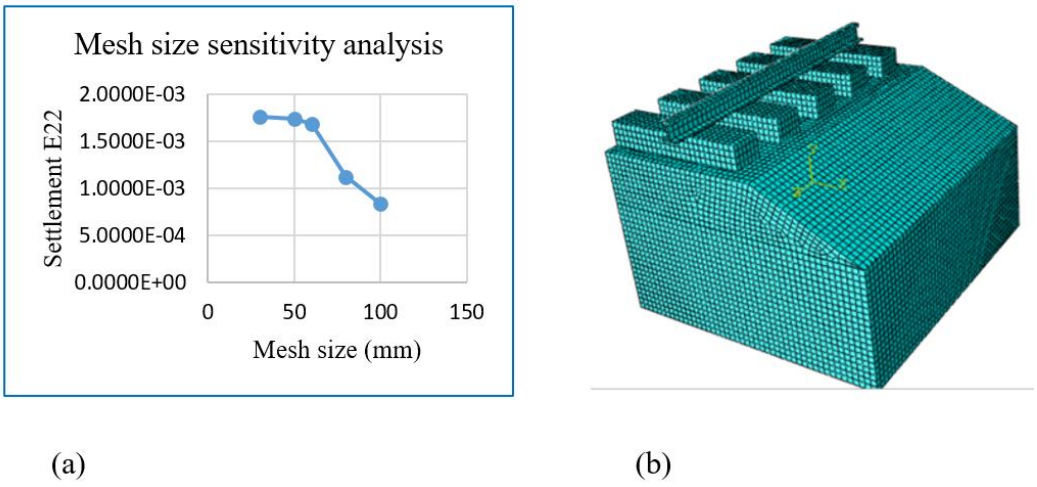

(a) (b)

Figure 3. 11 (a) Settlement-mesh size curve (b) 50 mm Meshed model

3.5.4 Boundary Conditions

The boundary conditions at both ends of the track were set fixing the displacement in the direction normal to the vertical surface (i.e., Z-symmetry) to simulate the continuity of the track. The bottom of the Ballast is set Encastre (U1=U2=U3=UR1=UR2=UR3=0) representing the structure below the track. The global coordinate system XYZ is defined as: The Z-axis is parallel to the longitudinal direction along which the wheel-set travels, the Y -axis is the vertical pointing upwards, and the X-axis is perpendicular to both Z and Y directions, which the rotational displacement is set, forming a right-handed Cartesian coordinate system.

3.6 Interaction of material surfaces in Abaqus

The fig 3.12 showing an interaction overview for material surfaces of part assembly in Abaqus

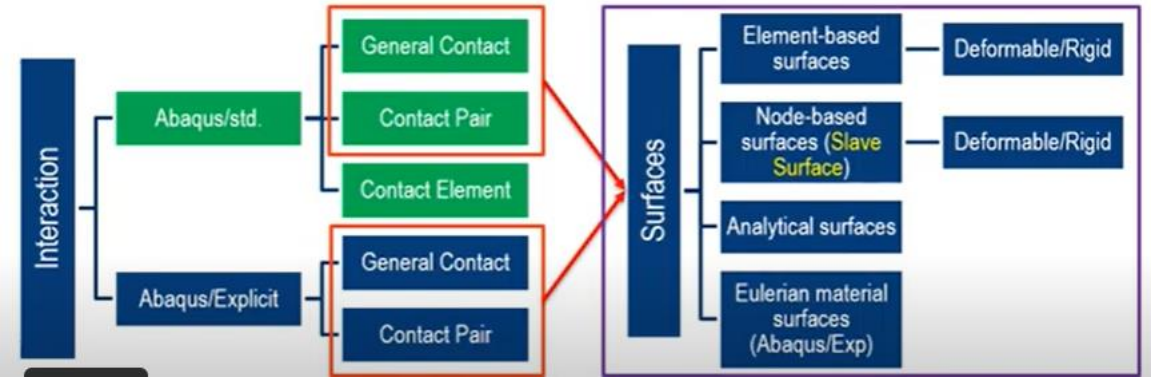

Figure 3. 12 Overview of material interaction in Abaqus [60]

3.6.1 Interaction surfaces

Interaction surfaces are used to; define contact, define regions and these regions prescribe distributed surface loads (traction, pressure, bolt load etc), tie dissimilar meshes together, define cavities used for cavity radiation analysis an Abaqus/standard, define pre-tensioned cavities, define sections for output quantities such as total force transmitted through a surface. There four most commonly used interaction surfaces in Abaqus as shown the fig 3.12 but the two basic ones are described briefly as follows;

- ❖ Element based-surfaces

They can be solid, structural, rigid, surface, gasket or acoustic elements, be defined by combination of elements of different part, be defined on the exterior or interior of anybody (e.g to define the cross section through a body).

- ❖ Node based-surfaces

Traditional “point-against-surface” method. Contact is enforced between a node and surface facet local to the node. The node is referred to as “slave” and the opposing surface is a “master” surface.

- ❖ Selecting Master/Slave surfaces

If you are going to define the interaction between two objects, then you have to define the master and slave surfaces on the following guiding principles; the larger of the two surfaces should act as master surface, if the surfaces are comparable in size, the stiffer surface body should act as the

master surface and if the surfaces are of comparable sizes and stiffness, a coarse mesh should act as the master surface

3.6.2 Contact

A contact interaction property can define tangential behavior (friction and elastic slip) and normal behavior (hard, soft, or damped contact and separation). Contact between two surfaces can become quite complex as it depends on many mechanical properties (and even thermal and electrical). Some mechanical properties include; tangential behavior (frictionless, rough and penalty), normal behavior, cohesive behavior, failure and damage evolution [60].

A contact interaction property can be referred to by a general contact, surface-to-surface contact, or self-contact interaction. For the case of General contact, Abaqus will use the same interaction property for all the possible surfaces in contact whereas surface to surface contact allows for defining particular interaction property for the specific surface contacts where necessary[60].

3.6.3 Constraint

The following types of constraints can be created currently on Abaqus [60];

Tie: A tie constraint allows you to fuse together two regions even though the meshes created on the surfaces of the regions may be dissimilar.

Rigid body: A rigid body constraint allows you to constrain the motion of regions of the assembly to the motion of a reference point.

Coupling: A coupling constraint allows you to constrain the motion of a surface to the motion of a single point.

3.6.4 Coefficient of friction at material contact interface

The coefficient of friction, μ, is a measure of the amount of friction existing between two surfaces. While defining the different interaction property for the tie constrains with regards to various surface contacts, the contact property options that were considered were mechanical tangential and normal contact behavior among several other properties. The normal property behavior was defined as “hard” contact which provides for non-penetration of the interfacing

surfaces and tangential property behavior provides for whether, during sliding of surfaces in contact, the contacts shall be rough (infinity coefficient of friction), frictionless or penalty (in between frictionless and rough). Given the unique material surfaces in the ballasted track model, the major varied parameter that differentiated the contact surfaces was coefficient of friction [70], [71].

The friction coefficient is known to be dependent on the surface condition, contact pressure and environmental conditions [72]. When looking in the literature, Coefficient of Friction (CoF) values in the range of 0.4 to 0.8 are typically used for DEM simulations of railway ballast, while more values of CoF are possible with cyclic tests [70]. Basing on this range of CoF values for ballast-ballast interface, the ballast-subgrade interface is assumed to be slightly lower and CoF of 0.4 was adopted for model input.

The steel-to-steel coefficient of friction to simulate the contact property between steel rail and steel wheel was adopted as 0.2. Additionally, the coated steel/coated steel dynamic coefficient of frictions in combinations with air is in the range between 0.14 and 0.42 with an influence of the amount of contact pressure [72]. The ballast-sleeper contact was adopted 0.5 whereas concrete to rubber and steel to rubber interfaces had CoF values of 0.6 and 0.35 respectively.

3.6.5 Type of contact for material interface used in modelling

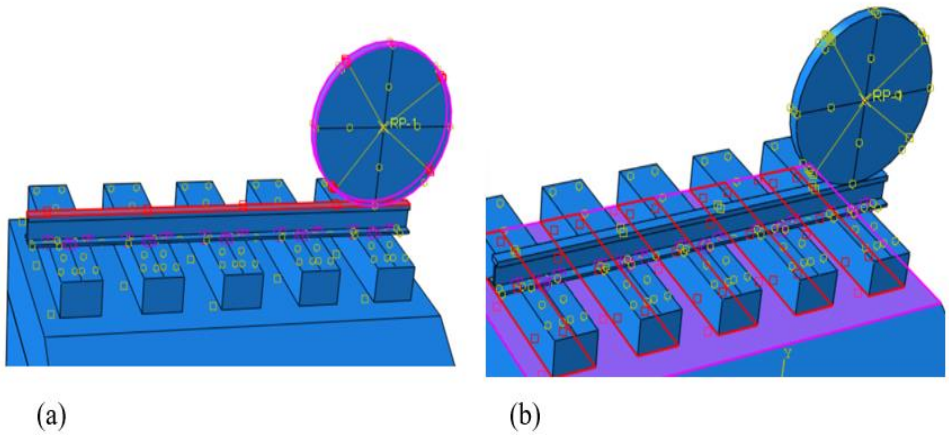

Figure 3. 13 Contact pair interaction and interaction property (a) wheel-rail surface to surface contact (b) sleeper-ballast surface to surface contact

For this thesis, the type of interaction adopted for interfacing was **contact pair** using element-based surfaces between the two material surfaces in contact. Contact pair interaction in Abaqus software allows for flexibility to define a unique interaction property for the different surfaces in contact within the model. When an interaction property is defined, it is applied between two surfaces (master and slave) as in fig 3.13.

The interaction details for the contact surfaces in the ballasted track model are summarized in the table 3.6.

Table 3.6 Model component material surface interface

Element Interface	**Type of Interaction**	**Interaction Property; Mechanical properties**	
		Tangential behavior CoF (Penalty method)	Normal contact behavior
Subgrade-ballast	Contact pair	0.40	"Hard" contact
Ballast-sleeper	Contact pair	0.50	"Hard" contact
Sleeper-rail pad	Contact pair	0.60	"Hard" contact
Rail pad-rail	Contact pair	0.35	"Hard" contact
Rail-wheel	Contact pair	0.20	"Hard" contact

The friction is created in the model by only specifying the coefficient of friction using penalty method and the software does the necessary interface solutions attributed the coefficient of friction.

3.7 Analysis type

3.7.1 General Static Analysis

The general static analysis can involve both linear and nonlinear effects and is performed to analyze static behavior such as deflection due to a static load. A criterion for the analysis to be possible is that, it is stable. A static step uses time increments, not in a manner of dynamic steps but rather as a fraction of the applied load. The default time period is 1.0 units of time, representing 100% of the applied load.

The nonlinear effects are expected, such as large displacements, material nonlinearities, boundary nonlinearities, contact or friction, the NLGEOM command should be used.

3.7.2 Dynamic Implicit Analysis

The dynamic implicit analysis method is used to calculate the transient dynamic response of a structure. A direct-integration dynamic analysis in Abaqus/Standard must be used when nonlinear dynamic response is being studied. The general direct-integration method provided in Abaqus/Standard, called the Hilber-Hughes-Taylor operator, is an extension of the trapezoidal rule. The half-step residual is the equilibrium residual error halfway through a time increment, $t + \Delta t/2$ and once the solution at $t + \Delta t$ has been obtained, the accuracy of the solution can be accessed and the time step adjusted appropriately [60]. This nonlinear equation solving process is expensive; and if the equations are very nonlinear, it may be difficult to obtain a solution. However, nonlinearities are usually more simply accounted for in dynamic situations than in static situations because the inertia terms provide mathematical stability to the system; thus, the method is successful in all but the most extreme cases. The choice of the time increment depends on the type of analysis performed.

In dynamic problems, a smaller time increment than the stable one might be used, to get an accurate result depending on the variations in the structure. There are two ways of defining the time increment: automatic or fixed incrementation [60]. The automatic incrementation scheme is provided for use with the general implicit dynamic integration method. The scheme uses a half-step residual control to ensure an accurate dynamic solution. By defining initial, minimum, and maximum increment sizes the automatic time increments can be chosen. If no convergence is achieved, a smaller one is used until convergence is achieved, down to the minimum increment defined [47].

3.7.3 Basis for choosing rail pad stiffness range of values used in the study

This process was guided by the range of rail pad stiffness that have been used for previous studies as follows;

- The most favorable rail pad stiffness for a conventional German line which was presented by a section with rail pads with stiffness equal to 27 kN/ mm, followed by 60 kN/mm pads, and finally 500 kN/mm pads (range of 60 to 500 kN/mm rail pad stiffness) [9].
- Sensitivity analysis on the stiffness of existing rail pads through track-train interaction modeling used a range of 50 to 250 kN/mm rail pad stiffness [11].

- Jabbar Ali Zakeri1 (2020) [19] on studying the influence of rail pad stiffness and axle loads on dynamic of train-track interaction used 60 to 240 kN/mm rail pad stiffness
- A rail pad with a stiffness of 1,300 kN/mm would reduce track stiffness by 4%, which corresponds to a reduction in track modulus by 5.3% and an increase in characteristic length by 1.4%. Thus, very stiff pads would have little effect on the track modulus and the characteristic length (i.e., load distribution) and therefore also on ballast pressure. It is of little use to use a very stiff pad that does not increase the characteristic length appreciably [2]
- In 1999, Ilias studied the influence of rail pad stiffness on wheelset-track interaction and corrugation growth (from 500 MN/m to 60 MN/m) [18]

Basing on the above background and from many other literatures suggesting use of soft rail pads mostly with stiffness below 100 kN/mm, a range of 50 to 1000 kN/mm rail pad stiffness was selected for study analysis in this thesis.

3.8 Selection of rail pad stiffness

Rail pad stiffness selection was achieved based on two parameters of reducing excessive rail vertical displacement and sleeper vertical acceleration. The parameters could be more than these highlighted basing on the outputs of varying rail pad stiffness in the study, however, rail acceleration, stress and rail seat loads were having a similar trend change or were dependent on rail displacement.

Weighted sum method was used where the sleeper vertical acceleration was associated with track safety and given a weighted coefficient of 59% while the rail vertical displacement was associated with cost and given weighted coefficient of 41%. The coefficient values were guided by studies of Jonan Backman (2002) [52] in his study.

3.8.1 Objective functions

Whereas the discussion above considers the significance of weights in terms of an optimal set, this section focuses on the relationship between a set of weights and the objective function values [73]. First, consider a problem with two unconstrained objective functions:

$$U = W_1F_1(x) + W_2F_2(x) \qquad \text{eq 3.1}$$

For U to have a minimum, it is necessary that, the gradient of U is equal to zero as follows

$$\Delta_x U = W_1 \Delta_x F_1 + W_2 \Delta_x F_2 = 0 \qquad \text{eq 3.2}$$

Assuming the weights are positive and noting that minimizing a weighted sum always provides an optimal solution [73], eq 3.2 indicates that at an optimal point, the gradients of the two objective functions are co-linear and point in opposite directions. Essentially, the linear combination of the gradients equals zero. In compliance with the definition optimality, this suggests that moving from a solution that satisfies eq 3.2, in order to improve a function, is detrimental to at least one other function.

4.0 RESULTS AND DISCUSSION

In chapter three, the ballasted track component's dimensions were selected and the corresponding geometry, material property, elements and parameters used in modelling were highlighted. In this chapter, the results for both static and dynamic analysis of ballasted track are presented in reference to the objectives of this study.

4.1 Results for Static Analysis

Under static analysis, two case scenarios of loading were analyzed; when the wheel load is directly on top of sleeper and when it is at the mid-point between sleepers. The track vertical responses (rail displacement and stress) and rail seat loads were the analyzed out puts. However, the rail seat loads could not be read directly from the simulation analysis but alternatively, it was calculated using Classic approach-Talbot formular with rail displacement as the input. The table 4.1 shows the rail displacement and stresses for the two loading scenarios.

Table 4.1 Rail vertical displacement and stresses for the two loading scenarios (wheel load directly on top of sleeper and at mid-point between sleepers)

Rail pad stiffness (kN/mm)	**wheel load between sleepers**		**wheel load directly on top of sleeper**	
	Rail vertical displacement (mm)	Rail vertical stress (MPa)	Rail vertical displacement (mm)	Rail vertical stress (MPa)
50	1.0084	74.366	0.95645	71.235
100	0.7987	78.865	0.74516	78.182
150	0.6389	81.849	0.57387	82.660
200	0.5251	84.850	0.48512	85.765
250	0.4695	86.995	0.43323	87.676
300	0.4392	90.995	0.40490	89.910
400	0.4069	94.951	0.38212	92.190
500	0.3957	95.833	0.36520	93.675
1000	0.3424	98.417	0.29240	96.740

4.1.1 Rail vertical stress with loading on top of sleeper

In ABAQUAS software, stresses are obtained as mises, principal and directional stresses. For this study, directional stress in vertical direction (S22) was considered for the different rail pad stiffness as presented fig 4.1.

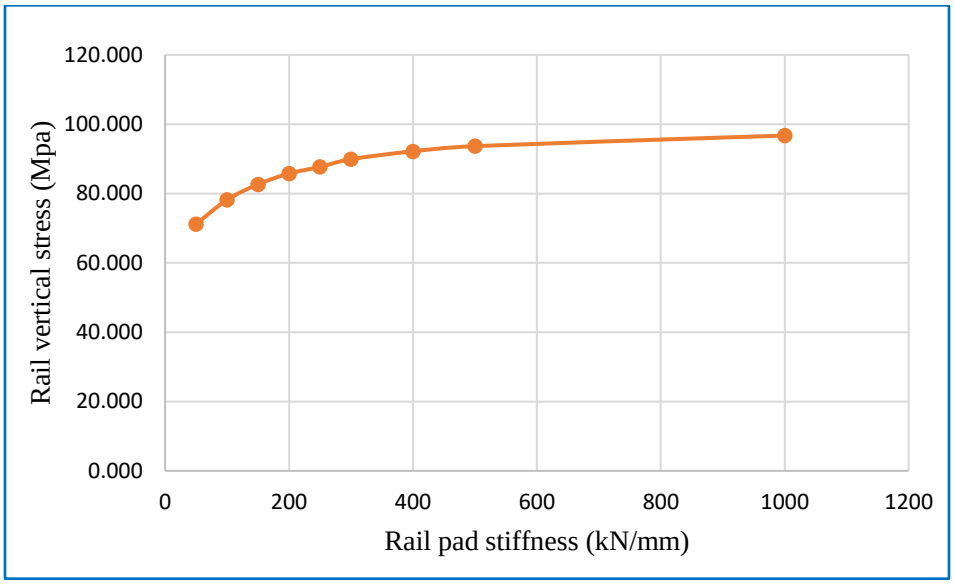

Figure 4. 1 Rail stress variation with wheel load directly on top sleeper

Generally, there was an observed increase in stress with increase in rail pad stiffness. The increase from 50 kN/mm to 150 kN/mm is very steep, it then becomes less steep gradually up to 400 kN/mm and finally the stress curve slope tends to flatten until 1000 kN/mm rail pad stiffness. The results show that, beyond rail pad stiffness of 200 kN/mm, the impact of increasing the rail pad stiffness on the rail stress begins to decline considerably.

The percentage stress increment at 200 (20%), 300 (30%) and 500 (50%) kN/mm rail pad stiffness is 57%, 73% and 88%. As the rail pad stiffness increases, more coupling between the rail and the sleeper is achieved which limits free movement of rail hence increased stress.

According to Miguel Sol-Sánchez et al (2014) [9], replacing stiff rail pads (250 kN/mm with 40 kN/mm) reduced stresses transmitted to the sleeper by up to 20% in a ballasted track. From fig 4.1, reducing rail pad stiffness from 250 to 50 kN/mm reduces rail stress from 88 MPa to 71 MPa (19%) and hence a good comparison.

4.1.2 Vertical displacement with loading on top of sleeper

The rail vertical displacement decreases as the rail pad stiffness is increased. This is because, the increase in rail pad stiffness increases rail-sleeper coupling and limits the possible rail flexibility and hence reduced displacement as illustrated in the fig 4.2.

There is a general decline in vertical rail displacement with increasing rail pad stiffness. However, the behavior of the curve keeps changing; from 50 kN/mm to 150 kN/mm rail pad stiffness, the curve is very steep and after 150 kN/mm rail pad stiffness and beyond, the curve becomes less steep and tends flatter beyond 500 kN/mm rail pad stiffness. The percentage reduction in rail displacement at 20%, 30% and 50% increase in rail pad stiffness is 71%, 83% and 89%.

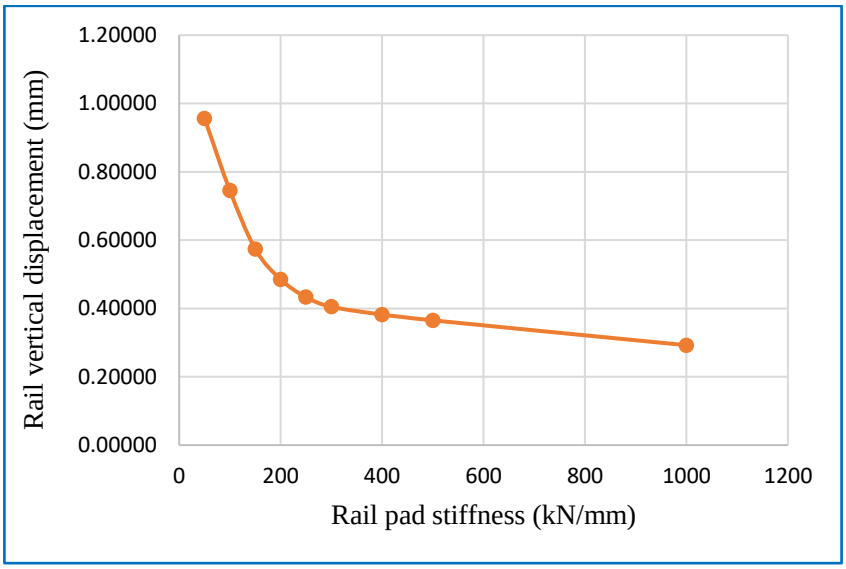

Figure 4. 2 Vertical rail displacement with wheel load directly on top of sleeper

At 20% increment in rail pad stiffness, the decrease in rail vertical displacement is 71% and compares exactly with the decrease in rail displacement according to X. Song et al (2020) [13]. Whereas at 50% increase in rail pad stiffness, there was 89% reduction in rail vertical displacement, which is in a fair agreement compared to Jabbar Ali Zakeri1 et al (2020) [19] where 50% increment in rail pad stiffness resulted into 80% reduction in rail vertical displacement. Also, Xiaolin Song (2020) [18] 50% increment in rail pad stiffness resulted into 83% reduction in rail vertical displacement. The difference can be attributed to non-exact track parameters used during modelling.

4.1.3 Rail seat loads loading on top of sleeper

Recall; the formulas below from chapter two.

$$x_1 = = \frac{\pi}{4} \left(\frac{4EI}{k}\right)^{0.25}$$

Classic approach-Talbot formula for calculating rail seat loads and track rail deflection;

Rail Seat Load: $Q_O = \frac{0.391PS}{x_1}$

The rail deflection at the wheel, w_m, caused by wheel load P, is obtained from simulation analysis at x=0 (point of load application) and is substituted in equation below to solve for track modulus k

$$k = \frac{1}{4}\sqrt[3]{\frac{P^4}{EIW_m^4}}$$

The k value is then substituted in the equation for calculation of x_1 and finally x_1 helps in solving the rail seat load Q_o. The calculations are solved in excel sheet and results are tabulated in table 4.2

The distance to the position of zero deflection from point of maximum deflection, x_1 [48]

$$x_1 = \frac{\pi}{4} \left(\frac{4EI}{u}\right)^{0.25} \quad \text{eq 2.13}$$

The deflection value read from simulation w_m [49]

$$w_m = \frac{P\beta}{2K} = \frac{P\sqrt[4]{\frac{K}{4EI}}}{2K} \quad \text{eq 2.14}$$

Solving for Track modulus k, the only unknown, yields [49]

$$k = \frac{1}{4}\sqrt[3]{\frac{P^4}{EIW_m^4}} \quad \text{eq 2.15}$$

Rail Seat Load: $Q_O = 0.391PS/x_1$ eq 2.16

Where; P is the wheel load and

S is the sleeper spacing.

Table 4.2 Corresponding rail seat loads when the when load is directly on top of sleepers

Rail pad Stiffness (kN/mm)	Rail displacement w_m (mm)	Wheel load, P (N)	EI (Nmm^2)	Track modulus, k (N/mm^2)	x_1 (mm)	Rail seat load (N)
50	0.95645	125000	4.473E+12	100.6323	510.00	47916.66
100	0.74516	125000	4.473E+12	140.3743	469.28	52074.38
150	0.57387	125000	4.473E+12	198.8546	430.15	56811.48
200	0.48512	125000	4.473E+12	248.7835	406.72	60083.82
250	0.43323	125000	4.473E+12	289.2871	391.67	62392.79
300	0.40490	125000	4.473E+12	316.5848	382.94	63815.28
400	0.38212	125000	4.473E+12	341.9957	375.62	65058.99
500	0.36520	125000	4.473E+12	363.2838	369.99	66048.61
1000	0.29240	125000	4.473E+12	488.6342	343.56	71129.24

The results in table 4.2 are illustrated in fig 4.3. There is a sharp rise in rail seat loads at the initial increment of rail pad stiffness up to around 150 kN/mm rail pad stiffness and at 200 kN/mm, noticeable gradient change is seen. Beyond 500 kN/mm rail pad stiffness, the RSL rate of increase declines gradually. The percentage of RSL increment at 20%, 30% and 50% rail pad stiffness are 52%, 68% and 78%.

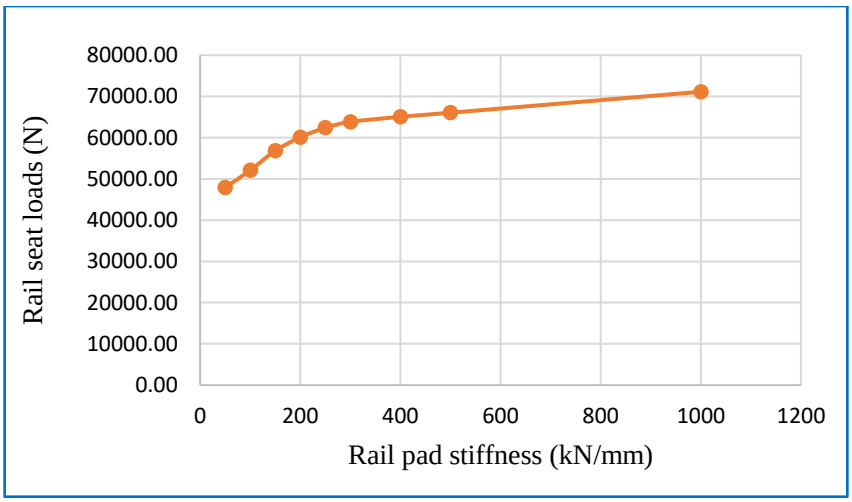

Figure 4. 3 showing Variation of rail seat loads with rail pad stiffness when the wheel load is directly on top of sleeper

Since rail seat loads change in the same proportion to stress transmitted to the sleeper (taking constant rail seat area). The reduction in rail pad stiffness from 250 to 50 kN/mm reduces rail seat loads from 62393 N to 47917 N (23%). This is equivalent to the percentage decrement in stress reaching the sleeper top surface and this compares well with the findings of Miguel Sol-Sánchez et al (2014) [9] that, replacing stiff rail pads (250 kN/mm with 40 kN/mm) reduced stresses transmitted to the sleeper by up to 20% in a ballasted track.

4.1.4 Rail stress with loading at mid-point between sleepers

Generally, as expected in fig 4.4, increasing rail pad stiffness increases the rail stress as the coupling between the rail and sleeper is increased with rail movement increasingly restricted. The percentage of rail vertical stress increment at 20%, 30% and 50% rail pad stiffness are 44%, 68% and 89%.

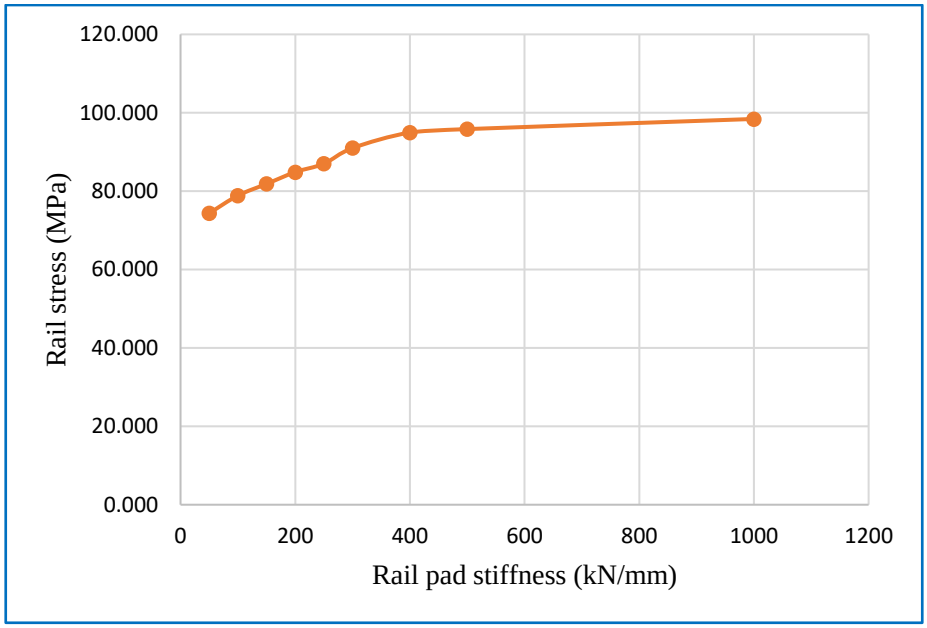

Figure 4. 4 Rail stress variation with wheel load at mid-point between sleepers

The discussion for this stress curve behavior with rail pad stiffness is similar to first scenario when the wheel load was directly on top of sleeper in section 4.1.1.

4.1.5 Rail vertical displacement with loading at mid-point between sleepers

Fig 4.5 illustrates that, the increase in rail pad stiffness leads to continuous reduction in the rail vertical displacement.

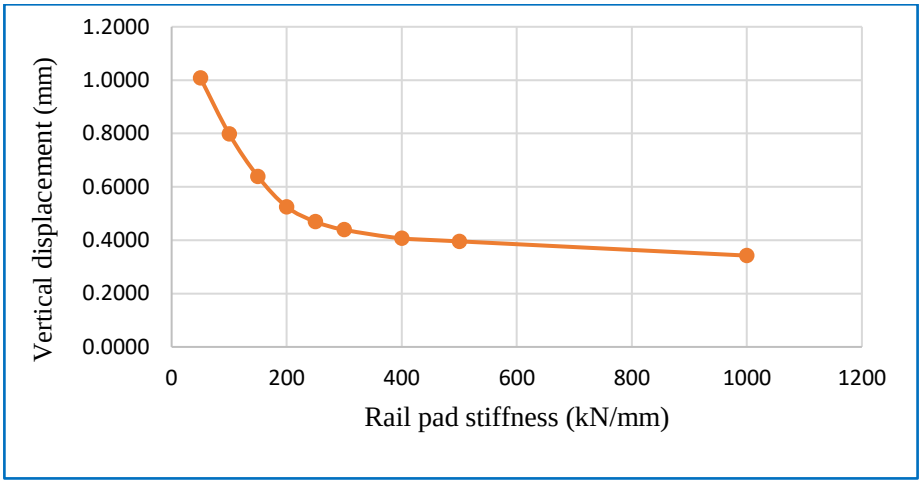

Figure 4. 5 Rail vertical displacement variation with load at mid-point between sleepers

Analysis of trend decrement of rail vertical displacement shows that, within 50 to 150 kN/mm rail pad stiffness, the slope of the graph is very steep and immediately changes significantly at 200 kN/mm rail pad stiffness tending flatter onwards as rail pad stiffness increases. The percentage of rail vertical displacement reduction at 20%, 30% and 50% rail pad stiffness are 73%, 79% and 92%.

As explained for the first loading scenario (wheel load is directly on top sleepers), similarly the maximum effect on rail vertical displacement reduction at 50% increase in rail pad stiffness is 92% which relatively compares with other researchers Jabbar Ali Zakeri1 (2020) [19] and Xiaolin Song (2020) [18].

Also at 20% rail pad stiffness increment, the observed 73% reduction in rail vertical displacement is in good agreement with X. Song (2020) et al [13], with 71% reduction in rail vertical displacement at 20% increment in rail pad stiffness.

4.1.6 Rail seat loads when loading is at mid-point between sleepers

The x_1, k and Q_o in table 4.3 are calculated from eq. 2.13, eq. 2.15 and eq. 2.16 respectively. The variation in RSLs with rail pad stiffness like in the first scenario (wheel load directly on top of sleepers), similarly in fig 4.6, RSLs variation with rail pad stiffness is quite similar. The percentage RSL increment at 20%, 30% and 50% rail pad stiffness are 56%, 74% and 84%.

Table 4.3 Rail seat loads when loading is at mid-point between sleepers

Rail pad Stiffness (kN/mm)	Rail displacement w_m (mm)	wheel load, P (N)	EI (Nmm2)	Track modulus, k (N/mm2)	X1 (mm)	Rail seat load (N)
50	1.0084	125000	4.473E+12	93.7799	519.07	47079.26
100	0.7987	125000	4.473E+12	127.9787	480.25	50884.63
150	0.6389	125000	4.473E+12	172.3362	445.82	54814.61
200	0.5251	125000	4.473E+12	223.8424	417.61	58517.77
250	0.4695	125000	4.473E+12	259.9022	402.30	60744.18
300	0.4392	125000	4.473E+12	284.0646	393.46	62109.27
400	0.4069	125000	4.473E+12	314.5323	383.56	63711.60
500	0.3957	125000	4.473E+12	326.3927	380.03	64303.90
1000	0.3424	125000	4.473E+12	395.8908	362.13	67483.25

The impact load reaching the sleeper top surface increases at considerably low rate after rail pad stiffness of 500 kN/mm to 1000 kN/mm as it was in the first loading scenario.

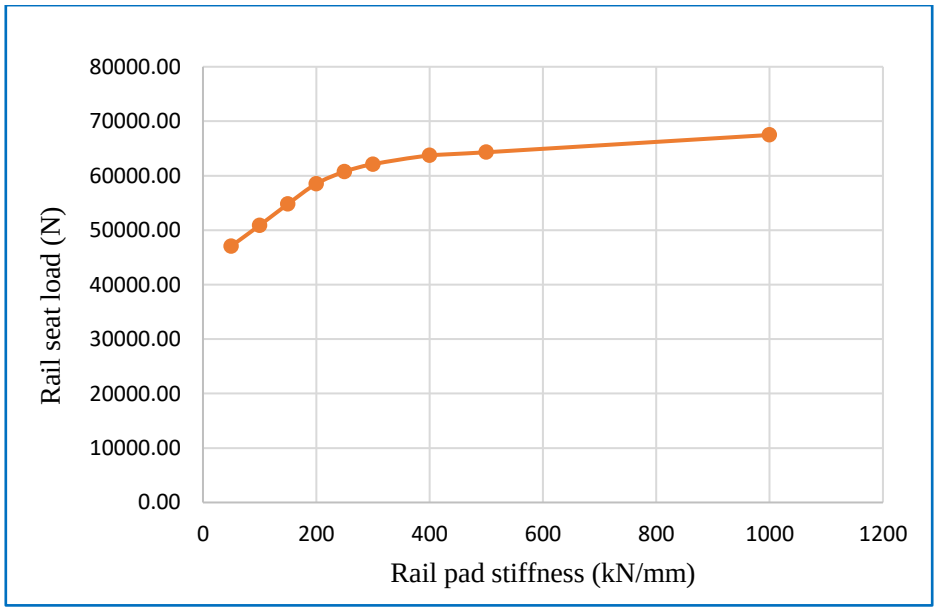

Figure 4. 6 Rail seat load variation when the load is at mid-point between sleepers

The result indicates that, there is equally no perceptible change in track stiffness and track modulus and this is in line with findings of Nazmul Hasan (2019) [2] that, it is of little use to use a very stiff pad (such as over 1300 kN/mm stiffness) that does not increase the characteristic length appreciably.

According to Miguel Sol-Sánchez et al (2014) [9], it was indicated that, a 20% reduction in sleeper stresses with rail pad stiffness was realized with reduction of rail pad stiffness from 250 kN/mm to 40 kN/mm, thus comparing well with the resulting stresses from RSLs for this study with a reduction of 22% sleeper stresses with rail pad stiffness reduction from 250 to 50 kN/mm.

4.2 Results for Dynamic Analysis

The results presented under this section of dynamic track analysis includes, vertical components of rail displacement, rail acceleration, sleeper acceleration and resulting rail seat loads. This is detailed in table 4.4.

Table 4.4 Results for rail vertical displacement, acceleration and sleeper vertical acceleration

Rail pad stiffness (kN/mm)	Rail displacement (mm)	Rail vertical acceleration (mm/s^2)	Sleeper vertical acceleration (mm/s^2)
50	0.32667	9.5786E+03	1.7226E+03
100	0.28902	9.2883E+03	1.9860E+03
150	0.26177	8.9852E+03	2.4262E+03
200	0.24013	8.8674E+03	2.6112E+03
300	0.21812	8.6989E+03	2.7280E+03
400	0.20622	8.6761E+03	2.9065E+03
500	0.19888	8.6520E+03	3.0360E+03
1000	0.19044	8.5440E+03	3.3313E+03

The maximum rail vertical acceleration from X. Song et al (2020) [13] was 11 m/s^2. Dynamic analysis of rail track for high-speed trains by A. Gomes Correia et al (2007) [74] using combination of commercial FEA software on ballasted railway track reported maximum rail

acceleration of 4.82 m/s^2 while estimations and measurements on the same track were as high as 45 m/s^2. Pranjal Mandhaniya et al (2022) [75] during FEA of vertical components of ballasted track responses including acceleration obtained maximum vertical acceleration of 8 m/s^2. Vertical peak rail acceleration of over 100 m/s^2 during the passage of vehicle on track at speed of 200 km/h in ballasted railway track has been reported by K Nguyen et al (2014) [76].

From table 4.4, the maximum rail vertical acceleration from this study was 9.58 m/s^2 which occurs at rail pad stiffness of 50 kN/mm and it is within the range of values obtained by other authors in the reviewed literature.

According to J. Choi et al (2014) [77] during qualitative analyses for dynamic behavior of railway ballasted track, the maximum values for sleeper acceleration recorded for soft, normal and stiff track were 12 m/s^2, 6 m/s^2 and 7 m/s^2 respectively. The highest sleeper acceleration value recorded during dynamic analysis of this study in table 4.4 was 3.33 m/s^2 which is good range for normal track stiffness.

The reasonable values of rail and sleeper vertical acceleration from this study is an assurance of the reliability of the FEA model of ballasted railway track that has been used.

4.2.1 Rail vertical displacement

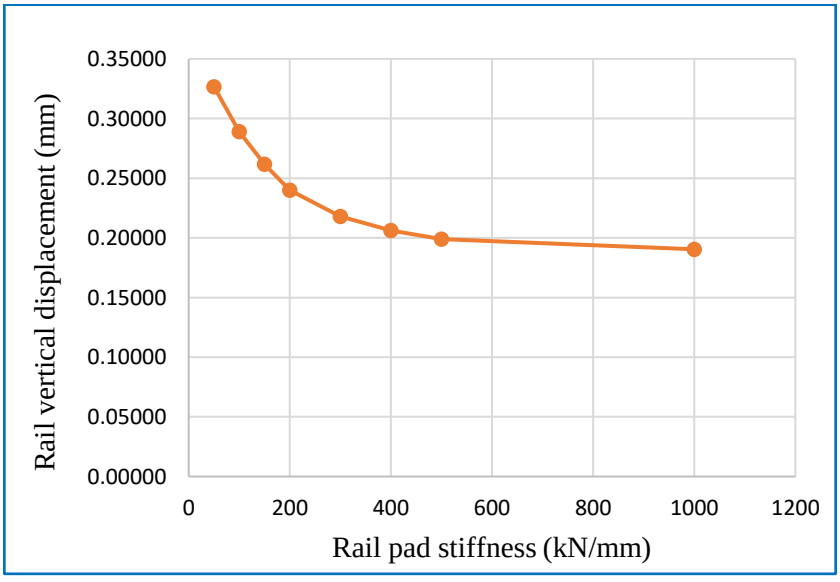

Figure 4. 7 Rail vertical displacement with variation with rail pad stiffness

With variation in rail pad stiffness, the respective rail vertical displacements (U2) were read from the visualization module provided in Abaqus. The rail vertical displacement as in fig 4.7 is reduced gradually with increase of rail pad stiffness from 50 to 500 kN/mm and after this point, the curve gradient becomes considerably less steep until 1000 kN/mm rail pad stiffness.

The increase in rail pad stiffness by 20%, 30% and 50% causes decrease in rail vertical displacement by 64%, 80% and 94% respectively. Since the rail vertical displacement variation with rail pad stiffness results for dynamic analysis, apart from change in magnitude show no much difference with results in static analysis case, the explanation for result comparison with other researchers is explained in section 4.1.2.

4.2.2 Rail vertical acceleration

The rail vertical acceleration decreases continuously with increase in rail pad stiffness until 500 kN/mm rail pad stiffness when the rate of change becomes less steep up to 1000 kN/mm rail pad stiffness.

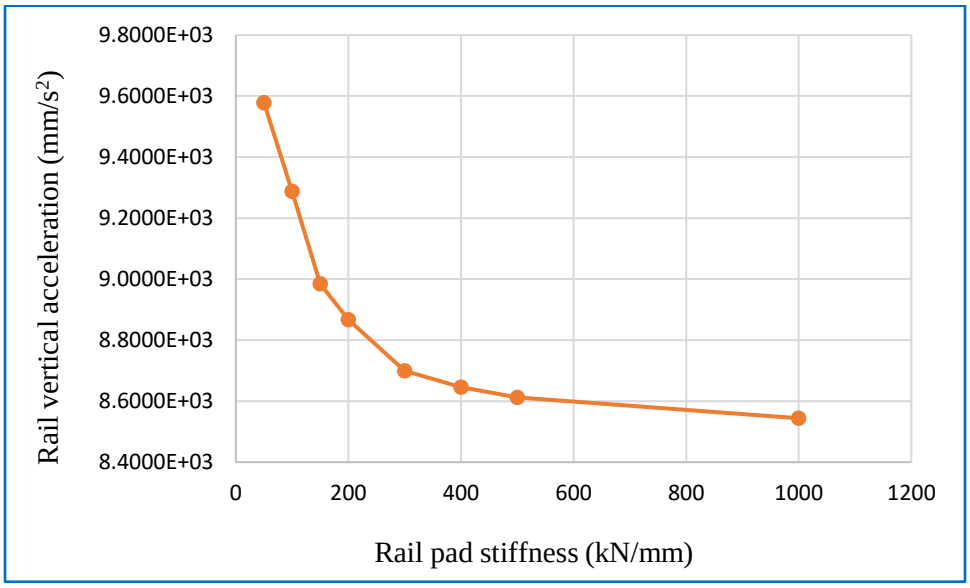

Figure 4. 8 Rail vertical acceleration variation with rail pad stiffness

The increase of rail pad stiffness by 20%, 30% and 50% causes decrease in rail vertical acceleration by 69%, 85% and 90% respectively. The rail coupling of the rail with the sleeper increases with rail pad stiffness and therefore, as it is in the case rail vertical displacement, the rail vertical acceleration decreases in a relatively similar trend.

4.2.3 Sleeper vertical acceleration

The sleeper vertical acceleration increases with a sharp gradient from 50 kN/mm to 150 kN/mm rail pad stiffness. The increase of rail pad stiffness by 20%, 30% and 50% causes an increase in sleeper vertical acceleration of 55%, 62% and 82% respectively.

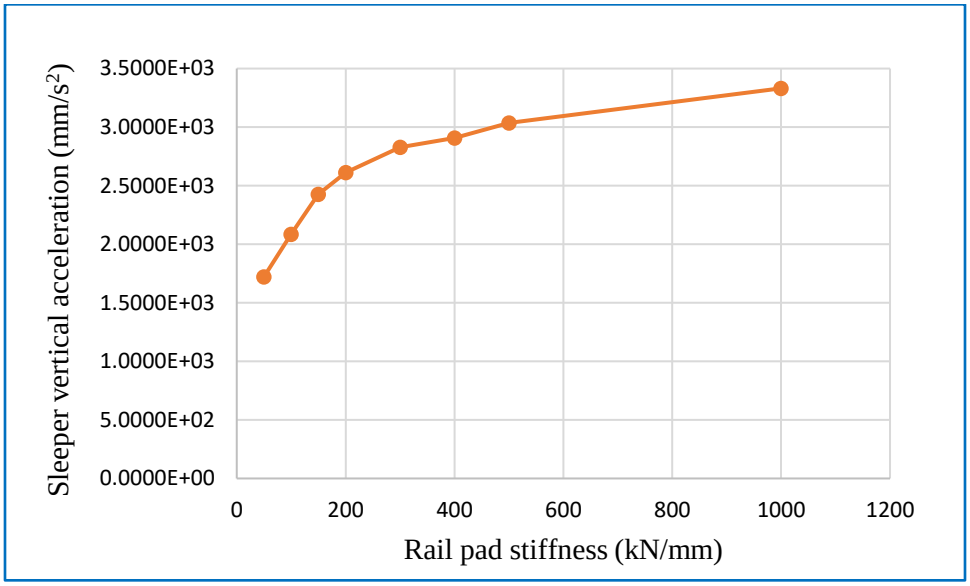

Figure 4. 9 variation of Sleeper vertical acceleration with rail pad stiffness

The results of sleeper vertical acceleration as per this study are comparable in trend with the findings obtained by Jabbar Ali Zakeri (2008) [11] with 71% increase in sleeper-ballast contact force (linked to sleeper vertical acceleration) at 50% rail pad stiffness.

Also, according to D. J Thompson et al (1999) [42], [33], the influence of rial pad stiffness on noise power level (linked to acceleration) shows an estimate of increase in sleeper acceleration of 79% when the rail pad stiffness increases from 25 to 250 (225) kN/mm. This fairly compares with this study where there was an observed increase in sleeper acceleration of 62% with increase in rail pad stiffness from 50 to 300 (250) kN/mm.

4.2.4 Rail seat loads (RSLs)

Arising from the rail vertical displacement (deflection), the track modulus, k values, distance X_1 from point of load application (maximum displacement) to zero deflection point. k and x_1 values are then used to obtain rail seat loads using talbot classic-approach formular. This was solved in excel and the results are shown in table 4.5.

The increase in rail seat loads is inversely proportional to rail vertical displacement. When the rail displacement is large, the loads are spread over more sleepers (reduced rail seat loads) and vice versa

Table 4.5 Rail seat loads variation with rail pad stiffness

Rail pad Stiffness	Rail displacement w_m (mm)	Wheel load, P (N)	EI (Nmm2)	Track modulus, k (N/mm2)	x_1 (mm)	Rail seat load, Q_o (N)
50	0.32667	125000	4.473E+12	421.5102	356.49	68549.48
100	0.28902	125000	4.473E+12	496.2683	342.24	71405.44
150	0.26177	125000	4.473E+12	566.3183	331.12	73801.86
200	0.24013	125000	4.473E+12	635.3677	321.74	75955.37
300	0.21812	125000	4.473E+12	722.2592	311.59	78428.78
400	0.20622	125000	4.473E+12	778.3579	305.82	79909.24
500	0.19888	125000	4.473E+12	816.8938	302.14	80880.45
1000	0.19044	125000	4.473E+12	865.5181	297.81	82058.05

A summary of results shows that increasing rail pad stiffness by 20%, 30% and 50% caused increase in RSLs by 37%, 55% and 91% respectively. It is seen that, at high rail pad stiffness, the increase in RSLs is less perceptible as there is over 90% RSL increment at 50% rail pad stiffness.

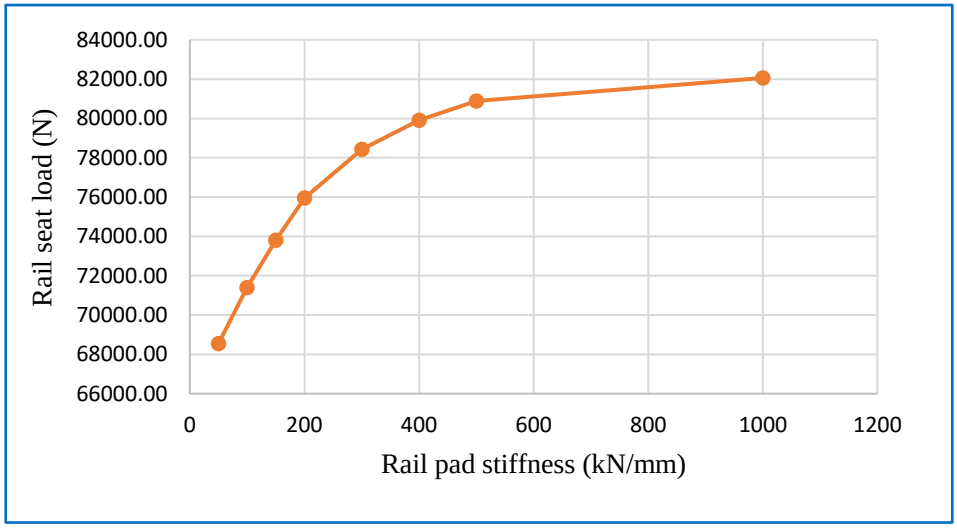

Figure 4. 10 Rail seat loads against rail pad stiffness

This is in agreement with Nazmul Hasan (2019) [2] with findings, that there little impact to use very stiff rail pads of over 1300 kN/mm rail pad stiffness.

4.3 Selection of best rail pad stiffness

For most of the different parameters studied with increase in rail pad stiffness, at 500 kN/mm rail pad stiffness (50% increase taking 1000 kN/mm as 100% rail pad stiffness for this study), it was observed that, the effect caused to most of the parameters was at least 70% to 90% increment or decrement depending on the parameter. This demonstrates that, up to 500 kN/mm rail pad stiffness, further increase in rail pad stiffness produces little impacts. Rail pad stiffness of lower than 500 kN/mm was recommended from this study to be considered in the selection.

The weighted sum method was used to select the best rail pad stiffness value that reduces on the rail vertical displacement and sleeper vertical acceleration using the weighting coefficients α_1 and α_2 representing 0.59 and 0.41 weighted coefficients. Therefore, comparison was considered in choosing between rail pad stiffness of 150 to 500 kN/mm.

It was noticed in most of the parameter variation with rail pad stiffness that, there was a sharp gradient between 50 to 100 kN/mm rail pad stiffness, and drastic gradient change at 150 kN/mm rail pad stiffness as most effects started declining with further increase in rail pad stiffness. A kind of curve transition is seen from 150 to 500 kN/mm rail pad stiffness and thus the basis for range of rail pad stiffness values as in table 4.6. The weighted sum of ranking for the two parameter outputs considering 150, 200, 300 and 500 kN/mm rail pad stiffness are 2.23, 2.41, 2.59, and 2.77 respectively

Table 4.6 Ranking for selection of most suitable rail pad stiffness

Rail pad stiffness (kN/mm)	Percentage decrement in rail vertical displacement	Ranking	Weighted ranking	Percentage increment in sleeper vertical acceleration	Ranking	Weighted Ranking	Sum of weighted Rankings
150	48	4	1.64	44	1	0.59	2.23
200	64	3	1.23	55	2	1.18	2.41
300	80	2	0.82	62	3	1.77	2.59
500	94	1	0.41	82	4	2.36	2.77

According R. Timothy Marler (2009) [73] minimizing a weighted sum always provides an optimal solution and from the above result, minimum weighted sum of ranking corresponds to 150 kN/mm rail pad stiffness. The rail pad stiffness of 150 kN/mm allows 48% reduction in rail vertical displacement compared to 28% decrement possible in 100 kN/mm rail pad stiffness and 44% increment in sleeper vertical acceleration compared to 16% for 100 kN/mm rail pad stiffness, all considering dynamic analysis (the speed used in the analysis was 90 Km/h).

Where more rail displacement reduction is desired due to other purposes, up to 200 kN/mm rail pad stiffness can be used that reduces rail vertical displacement by 64%, however this will allow 55% increase in sleeper vertical acceleration. Nazmul Hasan (2019) [2], considering a track stiffness range of 50–100 kN/mm recommended desirable stiffness of rail pad in the range of 116–256 kN/mm [2]. The recommendation of 150 kN/mm stiffness from this study is in compliant to the desired recommended range of 116–256 kN/mm [2].

The results of the simulation analysis in this paper were compared with other validated models which include;

- The influence of rial pad stiffness on noise power level (linked to acceleration) reported in M. Sol-Sánchez et al (2015) [9] and D. Rate (2015) [33] that shows an estimate of increase in sleeper acceleration of 79% when the rail pad stiffness increases from 25 to 250 (225 kN/mm). This fairly compares with this study where there is an observed increase in sleeper acceleration of 72% with increase in rail pad stiffness from 50 to 300 (250 kN/mm).
- Though the variables are not the same, but the behavior of the rail displacement and increase in rail pad stiffness for this study and X. Song et al (2020) [13] are identical as in figure 4.12. For example, at 20% increment in rail pad stiffness, the decrement in rail vertical displacement is 73% for this study as in fig 4.12 (b) whereas it is 77% (a) X. Song et al (2020) [13].

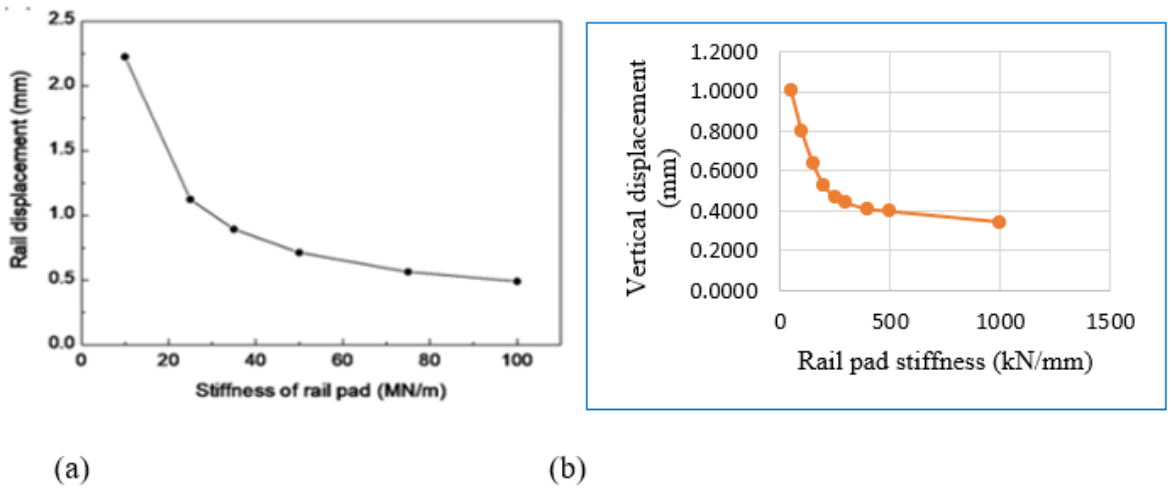

(a) (b)

Figure 4. 11 Rai displacement variation with stiffness of rail pad (a) X. Song (2020) [13] b) model used for study under static analysis

- According to J. Choi et al (2014) [77] during qualitative analyses for dynamic behavior of railway ballasted track, the maximum values for sleeper acceleration recorded for soft, normal and stiff track were 12 m/s^2, 6 m/s^2 and 7 m/s^2 respectively. The highest sleeper acceleration value recorded during this study was 3.33 m/s^2 which is good range for normal track stiffness.
- Additionally, the parameters used for ballasted track model preparation and analysis were obtained from validated model of a ballasted track section that was compliant with a laboratory experiment.

It is therefore concluded from the above background that, the model that has been used for this study is reliable as it compares fairly well with results of other researchers.

5.0 CONCLUSIONS AND RECOMMENDATIONS

5.1 Conclusions

Considering the many advantages of railways (efficiency, transportation capacity, low environmental impact, etc.), there are also some problems that require to be taken care of in order to improve their efficiency. Elastic elements are a suitable strategy to mitigate the associated track problems through dampening loads, vibrations and noises. The most commonly used elastic elements in railway infrastructure are rail pads, under-sleeper-pads, and under-ballast mats. This paper presents an analysis on the effect of rail pad stiffness on ballasted track behavior so as to select an appropriate rail pad stiffness to be applied in ballasted railway infrastructure to reduce the effect of the main problems associated with ballasted track.

In the present study, a 3D numerical analysis of ballasted railway track comprising rail, sleepers, ballast, subgrade and different stiffness of rail pad was conducted. To ensure preparation of a representative ballast track model, the material component parameters used were obtained from a model that replicated a ballasted track section and was validated using a laboratory experiment. The following results were drawn based on the investigations carried out;

Under static analysis and taking 1000 kN/mm rail pad stiffness as 100% increment, the increase in rail pad stiffness by 20%, 30% and 50% causes a reduction in rail vertical displacement by 73%, 79% 92% and 71%, 83%, 89%, causes an increase in rail vertical stress by 44%, 68% 89% and 57%, 73%, 88%, causes an increase in rail seat loads (RSLs) by 56%, 74%, 84% and 52%, 68%, 78% for the two loading scenarios of wheel load at mid-point between sleepers and directly on top of sleeper in all cases respectively.

Under dynamic analysis, the reduction in rail vertical displacement and rail vertical acceleration at 20%, 30%, 50% rail pad stiffness increment were 64%, 80%, 94% and 69%, 85%, 90% respectively. The increase in rail seat loads and sleeper vertical acceleration at 20%, 30% and 50% rail pad stiffness increment were 37%, 55% 91% and 55%, 62% 82% respectively.

Selection of rail pad stiffness was based on the criteria of rail vertical displacement and sleeper vertical acceleration using weighted sum averages of 0.41 and 0.59 respectively. The rail pad stiffness of 150 kN/mm which allows 48% reduction in rail vertical displacement and also 44%

increment in sleeper vertical acceleration under dynamic analysis has been recommended under this study. The basis of selecting rail pad stiffness was considering minimal weighted sum of ranking. Also, this was the rail pad stiffness at which the gradient for all parameter variations showed a clear change where the impact with further increase in rail pad stiffness declines perceptibly.

The selected rail pad stiffness under this study of 150 kN/mm is an agreement with recommendation of Nazmul Hasan (2019) [2], that the softest rail pad should not be less than 100 kN/mm and is defined to correspond to a 55% reduction in P_2 loads which are responsible for track degradation through ballast attrition and breakage. Considering a track stiffness range of 50–100 kN/mm, the recommended desirable stiffness is in the range of 116–256 kN [2] for which the recommendation of this study is compliant.

Even though some researchers recommend soft rail pads below 100 kN/mm rail pad stiffness, different studies have shown that soft rail pads (close to 80 kN/ mm) could increase rail movements (and thus its vibrations and noise) and deflection, which could cause the fatigue of other railway components. The finding of this paper fulfills the requirement of avoiding very soft rail pads below 100 kN/mm and recommends 150 kN/mm rail pad stiffness that mitigates the impacts of both excessive rail displacement and increased sleeper acceleration. The two output parameters are linked to drivers of track degradation and the findings of this study indirectly contributes to minimizing ballasted railway track degradation.

5.2 Recommendations

The following recommendations have been highlighted in this research study;

Since railway track routes are divided into straight section, curved section and transition section (between the straight and curved section and due to much variation in vehicle track forces at the transition and majorly in curved sections, the proposed rail pad stiffness may be less applicable in curved sections that are associated with changing track forces hence requiring different elastic elements to minimize the effects of highly varying loads at such track sections.

In this research, only the vertical wheel load was considered. The effect of other track loads such as lateral and longitudinal loads on rail pad stiffness were not considered. Therefore, future research that takes in account of these should be considered.

The interfacing elements at material surfaces in contact were assumed to be normal behavior "hard" contact with zero penetration of slave surface nodes into the master surface, however defining normal behavior "soft" which allows some penetration of the two surfaces in contact is an area for future consideration.

Correlation studies between reducing rail vertical displacement and increasing sleeper vertical acceleration with track degradation indicators should be an area for future research to quantify the possible achievement in minimization of track deterioration/degradation by use a specific rail pad stiffness.

REFEREENCES

[1] M. Sol-Sánchez, L. Pirozzolo, F. Moreno-Navarro, and M. C. Rubio-Gámez, "A study into the mechanical performance of different configurations for the railway track section: A laboratory approach," *Eng. Struct.*, vol. 119, pp. 13–23, 2016, doi: 10.1016/j.engstruct.2016.04.008.

[2] N. Hasan, "Rail Pad Stiffness and Classification System," *J. Transp. Eng. Part A Syst.*, vol. 145, no. 5, pp. 1–6, 2019, doi: 10.1061/jtepbs.0000231.

[3] R. Bullock and M. Lawrence, "Modern Railway Services in Africa: Building Traffic – Building Value," pp. 1–39, 2020, [Online]. Available: http://www.worldbank.org/transport

[4] I. Soleimanmeigouni, A. Ahmadi, and U. Kumar, "Track geometry degradation and maintenance modelling: A review," *Proc. Inst. Mech. Eng. Part F J. Rail Rapid Transit*, vol. 232, no. 1, pp. 73–102, 2018, doi: 10.1177/0954409716657849.

[5] M. A. Sayeed and M. A. Shahin, "Design of ballasted railway track foundations using numerical modelling. Part I: Development1," *Can. Geotech. J.*, vol. 55, no. 3, pp. 353–368, 2018, doi: 10.1139/cgj-2016-0633.

[6] N. Elkhoury, L. Hitihamillage, S. Moridpour, and D. Robert, "Degradation Prediction of Rail Tracks: A Review of the Existing Literature," *Open Transp. J.*, vol. 12, no. 1, pp. 88–104, 2018, doi: 10.2174/1874447801812010088.

[7] M. Burrow, P. F. Teixeira, T. Dahlberg, and E. Berggren, *Track stiffness considerations for high speed railway lines*, no. January. 2009.

[8] P. Ferreira, R. Maciel, J. Estaire, and M. Rodriguez-Plaza, "Railway track design optimisation for enhanced performance at very high speeds: experimental measurements and computational estimations," *Struct. Infrastruct. Eng.*, vol. 15, no. 1, pp. 1–13, 2019, doi: 10.1080/15732479.2018.1490325.

[9] M. Sol-Sánchez, F. Moreno-Navarro, and M. C. Rubio-Gámez, "The use of elastic elements in railway tracks: A state of the art review," *Constr. Build. Mater.*, vol. 75, pp. 293–305, 2015, doi: 10.1016/j.conbuildmat.2014.11.027.

[10] L. Puzavac, Z. Popović, and L. Lazarević, "Influence of Track Stiffness on Track Behaviour under Vertical Load," *PROMET - Traffic&Transportation*, vol. 24, no. 5, pp. 405–412, 1970, doi: 10.7307/ptt.v24i5.1176.

[11] J. A. Zakeri and H. Xia, "Sensitivity analysis of track parameters on train-track dynamic interaction," *J. Mech. Sci. Technol.*, vol. 22, no. 7, pp. 1299–1304, 2008, doi: 10.1007/s12206-008-0316-x.

[12] A. Remennikov and S. Kaewunruen, "Determination of dynamic properties of rail pads using an instrumented hammer impact technique," *Acoust. Aust.*, vol. 33, no. 2, pp. 63–67, 2005.

[13] X. Song, Y. Qian, K. Wang, and P. Liu, "Effect of Rail Pad Stiffness on Vehicle–Track Dynamic Interaction Excited by Rail Corrugation in Metro," *Transp. Res. Rec.*, vol. 2674, no. 6, pp. 225–243, 2020, doi: 10.1177/0361198120918584.

[14] M. I. H. Othman, A. M. A. Wahab, M. S. Hadi, and N. M. Noor, "Assessing the nonlinear static stiffness of rail pad using finite element method," *J. Vibroengineering*, vol. 24, no. 5, pp. 921–935, 2022, doi: 10.21595/jve.2022.22293.

[15] B. Lemma, "Analysis on the Influence of Rail Pad on Ballasted Railway Track," 2018.

[16] P. Musgrave and A. Stansfield, "Optimisation of Track Stiffness on the UK Railways The Journal July 2017 Volume 135 Part 3 please contact :," no. July 2017, 2020.

[17] V. Markine, A. De Man, and C. Esveld, "A Procedure for Design and Optimization of a Railway Track Structure," *Railw. Eng. TU Delft*, vol. 23, pp. 421–430, 2006, [Online]. Available: http://www.esveld.com/Download/TUD/Paris06.PDF

[18] J. I. Egana, J. Vinolas, and M. Seco, "Investigation of the influence of rail pad stiffness on rail corrugation on a transit system," vol. 261, pp. 216–224, 2006, doi: 10.1016/j.wear.2005.10.004.

[19] J. A. Zakeri, M. Fattahi, M. Nouri, and F. Janatabadi, "Influence of rail pad stiffness and axle loads on dynamic responses of train-track interaction with unsupported sleepers," *Period. Polytech. Civ. Eng.*, vol. 64, no. 2, pp. 524–534, 2020, doi: 10.3311/PPci.14826.

[20] C. A. Murray, W. Andy Take, and N. A. Hoult, "Measurement of vertical and longitudinal rail displacements using digital image correlation," *Can. Geotech. J.*, vol. 52, no. 2, pp. 141–155, 2015, doi: 10.1139/cgj-2013-0403.

[21] S. Kaewunruen and A. M. Remennikov, "Dynamic properties of railway track and its components: Recent findings and future research direction," *Insight Non-Destructive Test. Cond. Monit.*, vol. 52, no. 1, pp. 20–22, 2010, doi: 10.1784/insi.2010.52.1.20.

[22] E. T. Selig and J. M. Waters, "TRACK GEOTECHNOLOGY and SUBSTRUCTURE MANAGEMENT," *TRACK Geotechnol. Substruct. Manag.*, 1994, doi: 10.1680/tgasm.20139.

[23] K. Tzanakakis, *The LCC concept*, vol. 2. 2013. doi: 10.1007/978-3-642-36051-0_36.

[24] N. K. Kedia, A. Kumar, and Y. Singh, "Effect of Rail Irregularities and Rail Pad on Track Vibration and Noise," *KSCE J. Civ. Eng.*, vol. 25, no. 4, pp. 1341–1352, 2021, doi: 10.1007/s12205-021-1345-6.

[25] S. Kaewunruen and A. Remennikov, "Dynamic properties of railway track and its components: a state-of-the-art review," *New Res. Acoust.*, pp. 197–220, 2008, [Online]. Available: http://ro.uow.edu.au/cgi/viewcontent.cgi?article=1512&context=engpapers

[26] W. A. Siswanto, S. T. Yun, and W. M. Utomo, "Structural behavior of a ballasted small railway track under static and dynamic loadings," *Int. Rev. Model. Simulations*, vol. 7, no. 1, pp. 59–64, 2014.

[27] D. Li, S. Kaewunruen, and R. You, "Time-dependent behaviours of railway prestressed concrete sleepers in a track system," *Eng. Fail. Anal.*, vol. 127, no. i, 2021, doi: 10.1016/j.engfailanal.2021.105500.

[28] A. Y. Alemu, "Survey of Railway Ballast Selection and Aspects of Modelling Techniques," *Div. Highw. Railw. Eng. Div. Highw. Railw. Eng. Dep.*, pp. 1–61, 2011, [Online]. Available: http://urn.kb.se/resolve?urn=urn:nbn:se:kth:diva-87466

[29] C. Ngamkhanong, S. Kaewunruen, and C. Baniotopoulos, "A review on modelling and monitoring of railway ballast," *Struct. Monit. Maint.*, vol. 4, no. 3, pp. 195–220, 2017, doi: 10.12989/smm.2017.4.3.195.

[30] M. D. Project and H. Feng, "3D-models of Railway Track for Dynamic Analysis," 2011.

[31] M. Ito and K. Nagai, "Degradation issues of polymer materials used in railway field," *Polym. Degrad. Stab.*, vol. 93, no. 10, pp. 1723–1735, 2008, doi: 10.1016/j.polymdegradstab.2008.07.011.

[32] S. Lakusic, M. Ahac, I. Haladin, S. Lakušic, M. Ahac, and I. Haladin, "Experimental investigation of railway track with under sleeper pad," *Proc. 10th Slov. road Transp. Congr.*, no. October, pp. 386–393, 2010.

[33] D. Rate and D. Thompson, "Pad Stiffness," 2015.

[34] A. Fenander, "Frequency dependent stiffness and damping of railpads," *Proc. Inst. Mech. Eng. Part F J. Rail Rapid Transit*, vol. 211, no. 1, pp. 51–62, 1997, doi: 10.1243/0954409971530897.

[35] J. J. Heunis, "Material models for rail pads Material models for rail pads by".

[36] S. Kaewunruen and A. M. Remennikov, "Sensitivity analysis of free vibration characteristics of an in situ railway concrete sleeper to variations of rail pad parameters," *J. Sound Vib.*, vol. 298, no. 1–2, pp. 453–461, 2006, doi: 10.1016/j.jsv.2006.05.034.

[37] M. Sol-sánchez, F. Moreno-navarro, and M. C. Rubio-gámez, "Viability analysis of deconstructed tires as material for rail pads in high-speed railways," vol. 64, pp. 407–414, 2014, doi: 10.1016/j.matdes.2014.07.071.

[38] I. Grossoni, A. R. Andrade, Y. Bezin, and S. Neves, "The role of track stiffness and its spatial variability on long-term track quality deterioration," *Proc. Inst. Mech. Eng. Part F J. Rail Rapid Transit*, vol. 233, no. 1, pp. 16–32, 2019, doi: 10.1177/0954409718777372.

[39] K. Giannakos, "Influence of rail pad stiffness on track stressing, life-cycle and noise emission," *2nd Int. Conf. Sustain. Constr. Mater. Technol.*, no. January 2011, pp. 243–253, 2010.

[40] C. Wan, V. Markine, and I. Shevtsov, "Optimisation of the elastic track properties of turnout crossings," *Proc. Inst. Mech. Eng. Part F J. Rail Rapid Transit*, vol. 230, no. 2, pp. 360–373, 2016, doi: 10.1177/0954409714542478.

[41] L. Puzavac, Z. Popović, and L. Lazarević, "Uticaj krutosti šinske podloge na ponašanje koloseka pod vertikalnim opterećenjem," *Promet - Traffic - Traffico*, vol. 24, no. 5, pp. 405–412, 2012, doi: 10.7307/ptt.v24i5.1176.

[42] D. J. Thompson, C. J. C. Jones, T. Wu X, and G. De France, "The influence of the non-linear stiffness behaviour of rail pads on the track component of rolling noise," *Proc. Inst. Mech. Eng. Part F J. Rail Rapid Transit*, vol. 213, no. 4, pp. 233–241, 1999, doi: 10.1243/0954409991531173.

[43] A. M. Remennikov and S. Kaewunruen, "Progress in Structural Engineering and Materials : Structural Safety and Reliability A review of loading conditions for railway track structures due to train and track vertical interaction," no. October 2007, pp. 207–234, 2008, doi: 10.1002/stc.

[44] N. F. Doyle, "Railway Track Design: A Review of Current Practice Occasional Paper," *Bur. Transp. Econ. BHP Melb. Res. Lab.*, p. 303, 1980.

[45] National Research Council (U.S.). Transportation Research Board. *et al.*, *Railroad research issues.*, no. 1470. 1994.

[46] TSWG, *Cross Industry Track Stiffness Working Group - A Guide to Track Stiffness*. 2016.

[47] G. Started and I. Edition, "Getting Started with Abaqus: Interactive Edition".

[48] M. Fesharaki, "3-D Dynamic Analysis of High-Speed Railroad Track," 2017, doi: 10.25148/etd.FIDC001968.

[49] A. D. Kerr, "The determination of the track modulus k for the standard track analysis," *AREMA Annu. Conf.*, no. 1976, pp. 1–23, 2002.

[50] J. Sadeghi, "New Advances in Design of Railway Track System," *Reliab. Saf. Railw.*, 2012, doi: 10.5772/35903.

[51] J. Sadeghi and A. Hasheminezhad, "Sensitivity Analysis of Ballasted Railway Track Design Criteria," *3rd Int. Conf. Recent Adv. Railw. Eng.*, no. April 2013, 2013.

[52] J. Bäckman, *Railway Safety - Risks and Economics*. 2002. [Online]. Available: https://www.researchgate.net/publication/277828729_Railway_Safety_-

_Risks_and_Economics

[53] S. Kaewunruen, “An Experimental Evaluation of the Attenuation Effect of Rail Pad on Flexural Behaviour of Railway Concrete Sleeper under Severe Impact Loads An Experimental Evaluation of the Attenuation Effect of Rail Pad on Flexural Behaviour of Railway Concrete Sleeper,” 2008.

[54] A. Khajehdezfuly, “Effect of rail pad stiffness on the wheel/rail force intensity in a railway slab track with short-wave irregularity,” *Proc. Inst. Mech. Eng. Part F J. Rail Rapid Transit*, vol. 233, no. 10, pp. 1038–1049, 2019, doi: 10.1177/0954409718825410.

[55] X. Zhao *et al.*, “Determination of dynamic amplification factors for heavy haul railways,” *Proc. Inst. Mech. Eng. Part F J. Rail Rapid Transit*, vol. 232, no. 2, pp. 514–528, 2018, doi: 10.1177/0954409716679203.

[56] N. Submersibles, “Ue Re Next-Generation Submersibles Blade Cooling Car Wings,” vol. I, no. 1, 2007.

[57] M. Willford, R. Sturt, Y. Huang, I. Almufti, and X. Duan, “Recent advances in non-linear soil-structure interaction analysis using LS-DYNA,” 2007.

[58] M. Bayat, S. Eslamian, G. Shams, and A. Hajiannia, “The 3D analysis and estimation of transient seepage in earth dams through PLAXIS 3D software: neural network: Case study: Kord-Oliya Dam, Isfahan province, Iran,” *Environ. Earth Sci.*, vol. 78, no. 18, pp. 1–7, 2019, doi: 10.1007/s12665-019-8405-y.

[59] I. A. Magomedov and Z. S. Sebaeva, “Comparative study of finite element analysis software packages,” *J. Phys. Conf. Ser.*, vol. 1515, no. 3, 2020, doi: 10.1088/1742-6596/1515/3/032073.

[60] C. A. E. User, “Abaqus 6.14”.

[61] D. Joel, A. David, and J. D. Gardner, “Consortium on Deburring and Edge Finishing,” 2005.

[62] ANSYS, ANSYS Theory Guide, and ANSYS, “Theory Reference for the Mechanical APDL and Mechanical Applications,” *Ansys*, vol. 12, no. April, pp. 1–1226, 2009.

[63] M. J. Martínez-Echevarría, E. Tejeda, M. C. Rubio, and F. Moreno, “Evaluación del dispositivo pavement quality Indicator (PQI) en la determinación de la densidad in situ de mezclas fabricadas con emulsión bituminosa,” *Mater. Constr.*, vol. 63, no. 309, pp. 93–104, 2013, doi: 10.3989/mc.2013.03311.

[64] A. van Belkom, “A simplified method for calculating load distribution and rail deflections in track, incorporating the influence of sleeper stiffness,” *Adv. Struct. Eng.*, vol. 23, no. 11, pp. 2358–2372, 2020, doi: 10.1177/1369433220911144.

[65] A. de Bever, “Dynamic behaviour of rubber and rubberlike materials,” *WFW-report*, vol. 92.005, no. 1992, p. 15, 1992.

[66] K. Wang, Y. Zhuang, G. Kouretzis, and S. W. Sloan, “Shakedown analysis of ballasted track structure using three-dimensional finite element techniques,” *Acta Geotech.*, vol. 15, no. 5, pp. 1231–1241, 2020, doi: 10.1007/s11440-019-00818-6.

[67] T. Bose and E. Levenberg, “A Priori Determination of Track Modulus Based on Elastic Solutions,” *KSCE J. Civ. Eng.*, vol. 24, no. 10, pp. 2939–2948, 2020, doi: 10.1007/s12205-020-5372-5.

[68] M. Esmaeili, S. A. S. Hosseini, and M. Sharavi, “Experimental assessment of dynamic lateral resistance of railway concrete sleeper,” *Soil Dyn. Earthq. Eng.*, vol. 82, pp. 40–54, 2016, doi: 10.1016/j.soildyn.2015.11.011.

[69] H. M. El-sayed, H. N. Zohny, H. S. Riad, and M. N. Fayed, “A three-dimensional finite element analysis of concrete sleepers and fastening systems subjected to coupling vertical and lateral loads,” *Eng. Fail. Anal.*, vol. 122, no. September 2020, p. 105236, 2021, doi: 10.1016/j.engfailanal.2021.105236.

[70] B. Suhr, T. A. Butcher, R. Lewis, and K. Six, “This is a repository copy of Friction and wear in railway ballast stone interfaces . White Rose Research Online URL for this paper : Version : Published Version Article : Tribology International Friction and wear in railway ballast stone interfaces,” 2020.

[71] S. K. Navaratnarajah, H. G. S. Mayuranga, and S. Venuja, “Influence of Type of Sleeper–Ballast Interface on the Shear Behaviour of Railway Ballast: An Experimental and

Numerical Study," *Sustain.*, vol. 14, no. 24, 2022, doi: 10.3390/su142416384.

[72] R. J. M. Pijpers and H. M. Slot, "Friction coefficients for steel to steel contact surfaces in air and seawater," *J. Phys. Conf. Ser.*, vol. 1669, no. 1, 2020, doi: 10.1088/1742-6596/1669/1/012002.

[73] R. T. Marler and J. S. Arora, "The weighted sum method for multi-objective optimization: New insights," *Struct. Multidiscip. Optim.*, vol. 41, no. 6, pp. 853–862, 2010, doi: 10.1007/s00158-009-0460-7.

[74] A. Gomes Correia *et al.*, "Dynamic analysis of rail track for high speed trains. 2D approach," *Appl. Comput. Mech. Geotech. Eng. - Proc. 5th Int. Work. Appl. Comput. Mech. Geotech. Eng.*, pp. 461–472, 2007, doi: 10.1201/9781439833414.ch39.

[75] P. Mandhaniya, J. T. Shahu, and S. Chandra, "Analysis of Dynamic Response of Ballasted Rail Track Under a Moving Load to Determine the Critical Speed of Motion," *J. Vib. Eng. Technol.*, 2022, doi: 10.1007/s42417-022-00741-3.

[76] K. Nguyen, J. M. Goicolea, and F. Galbadón, "Comparison of dynamic effects of high-speed traffic load on ballasted track using a simplified two-dimensional and full three-dimensional model," *Proc. Inst. Mech. Eng. Part F J. Rail Rapid Transit*, vol. 228, no. 2, pp. 128–142, 2014, doi: 10.1177/0954409712465710.

[77] J. Choi, "Qualitative Analysis for Dynamic Behavior of Railway Ballasted Track," *PhD Diss. Berlin Inst. Technol. Berlin, Ger.*, no. Department of Track and Railway Operations, 2014.

APPENDICES

APPENDIX A: Static analysis results

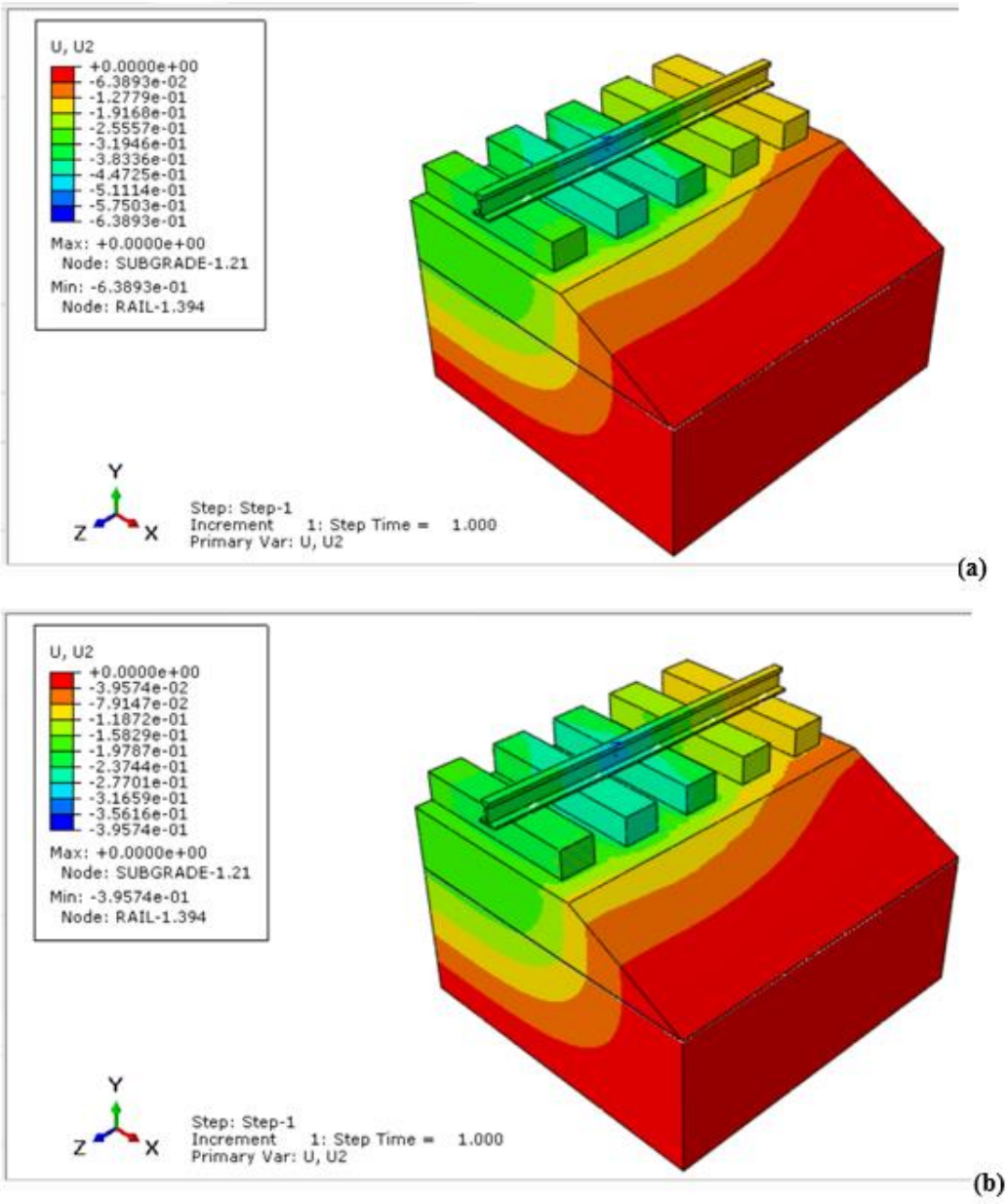

Figure A- 1 Rail vertical displacement at rail pad stiffness of (a) 150 kN/mm, (b) 500 kN/mm with wheel load at mid-point between sleepers

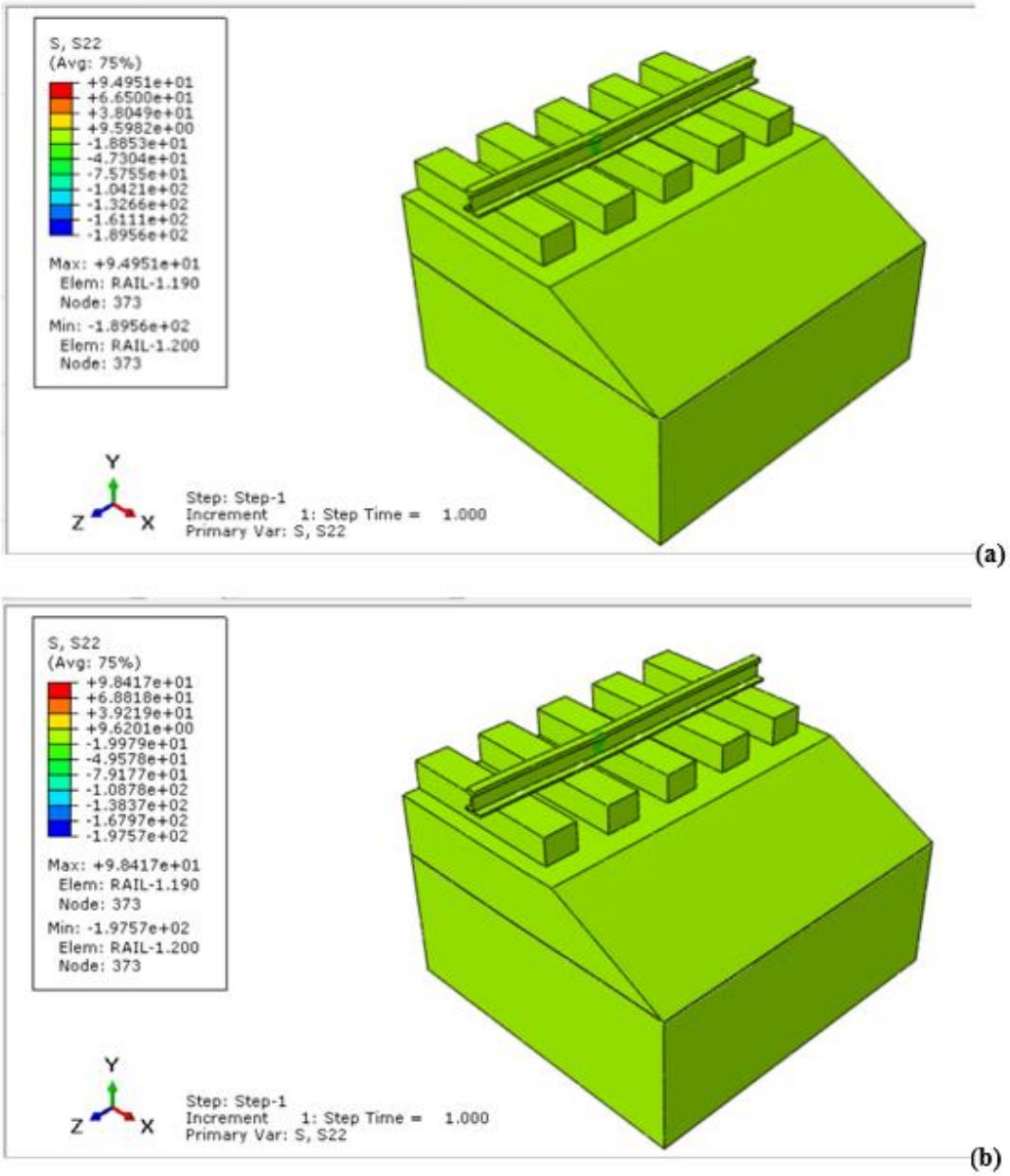

Figure A- 2 Rail vertical stress at rail pad stiffness of (a) 400 kN/mm and (b) 1000 kN/mm with wheel load at mid-point between sleepers

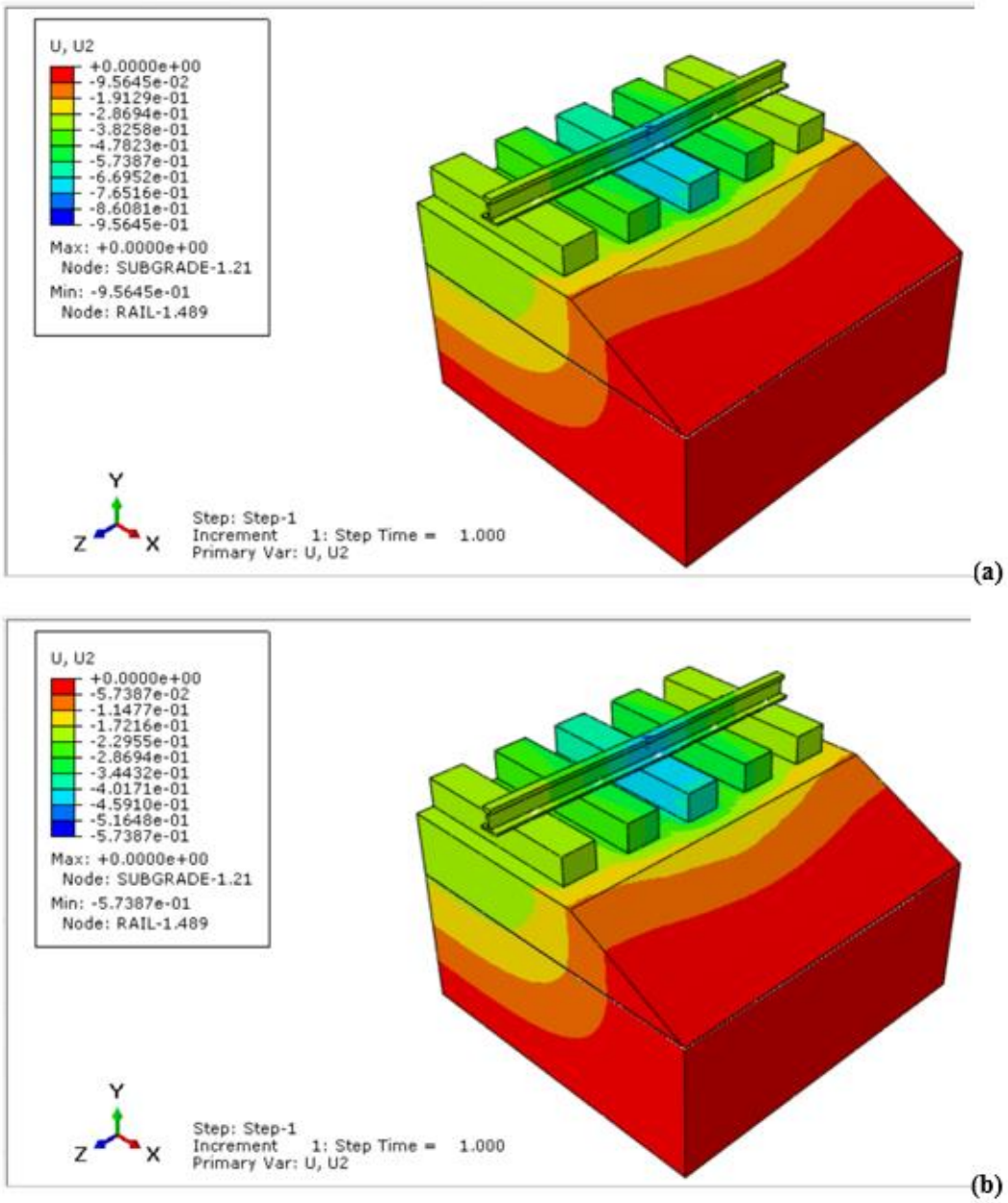

Figure A- 3 Rail vertical displacement at rail pad stiffness of (a) 50 kN/mm, (b) 150 kN/mm with wheel load is directly on top of sleeper

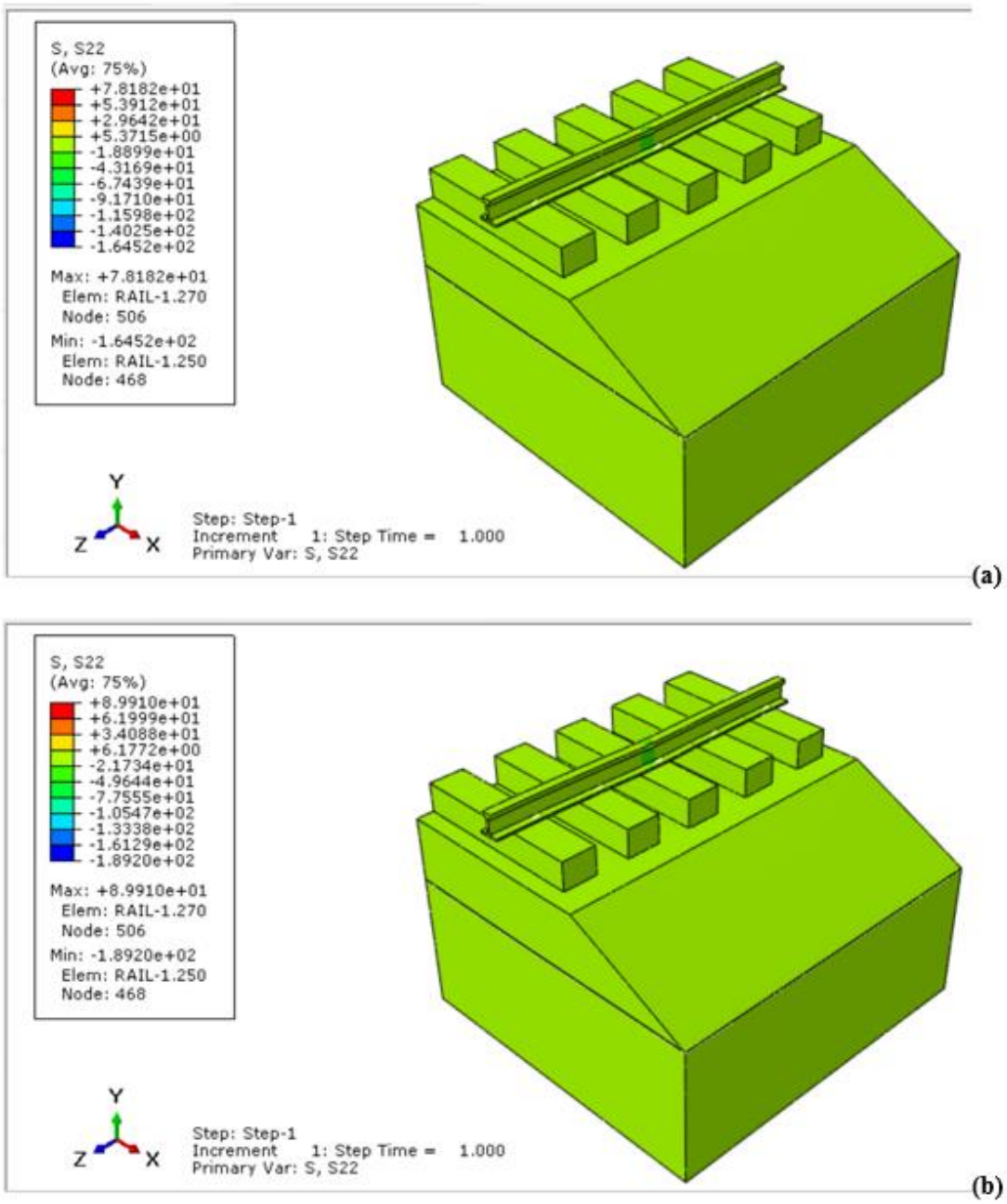

Figure A- 4 Rail vertical stress at rail pad stiffness of (a) 100 kN/mm and (b) 300 kN/mm with wheel load is directly on top sleepers

APPENDIX B Dynamic analysis results

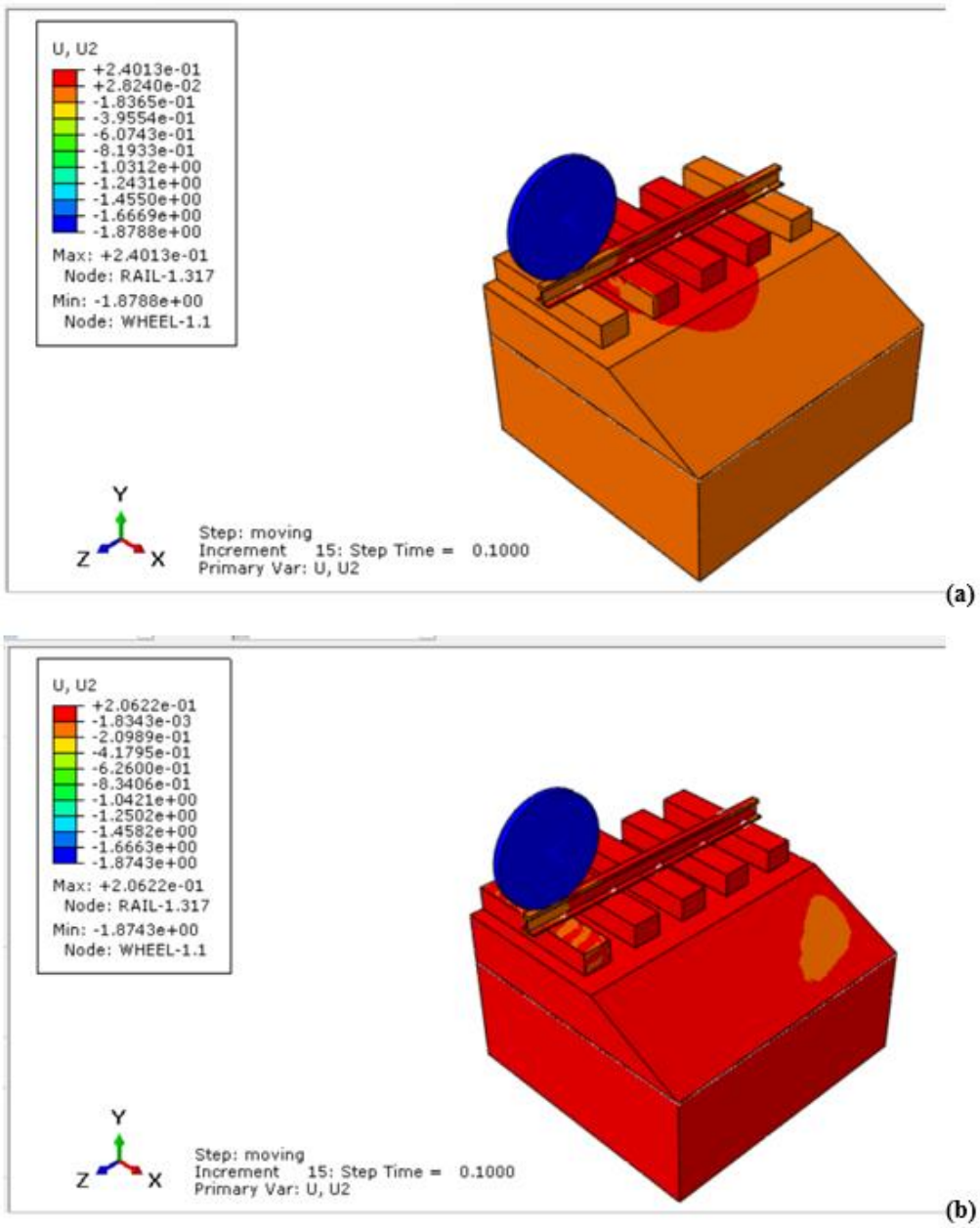

Figure B- 1 Rail vertical displacement at rail pad stiffness of (a) 200 kN/mm and (b) 400 kN/mm

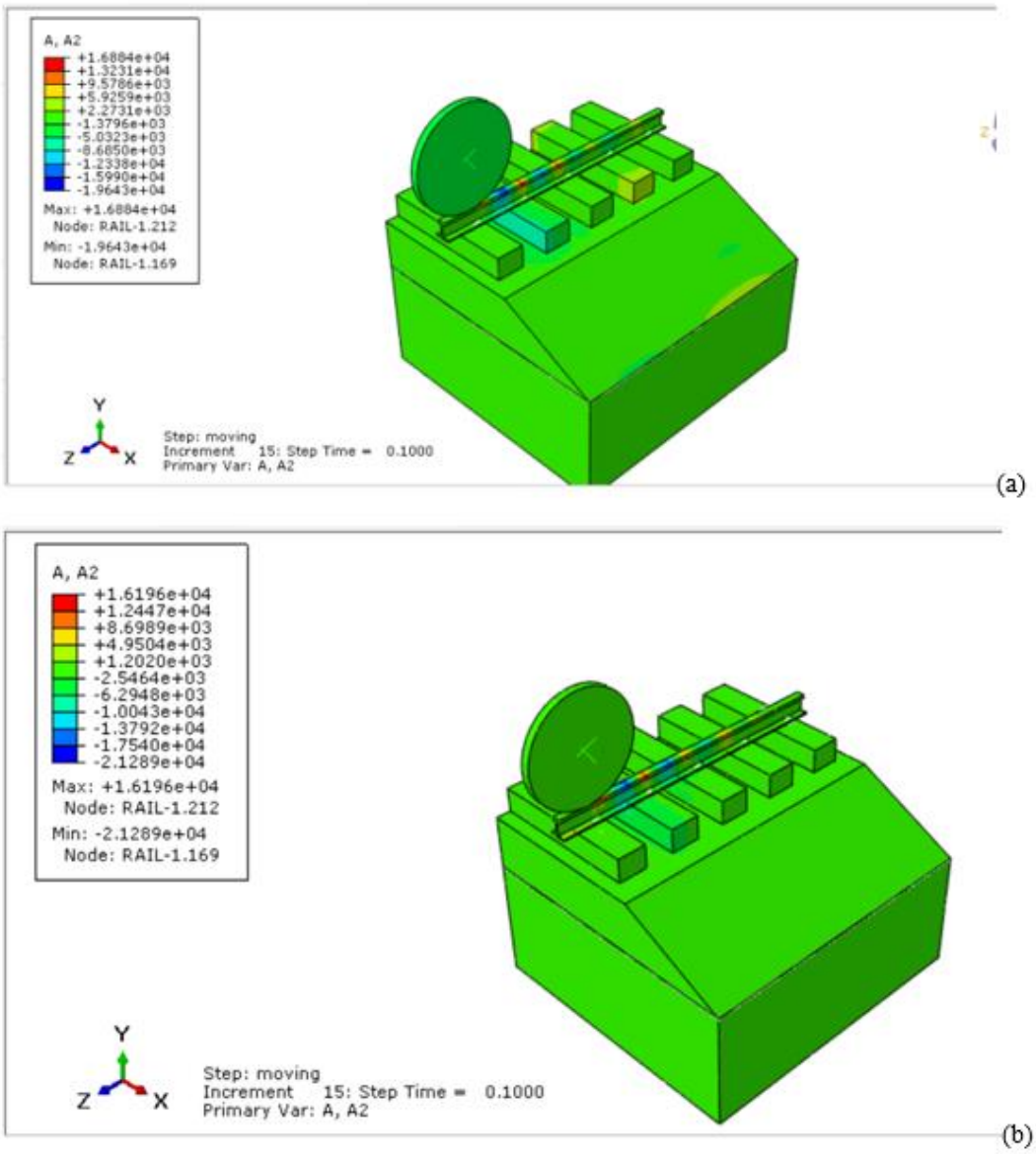

Figure B- 2 Rail vertical acceleration at rail pad stiffness of (a) 50 kN/mm (b) 300 kN/mm

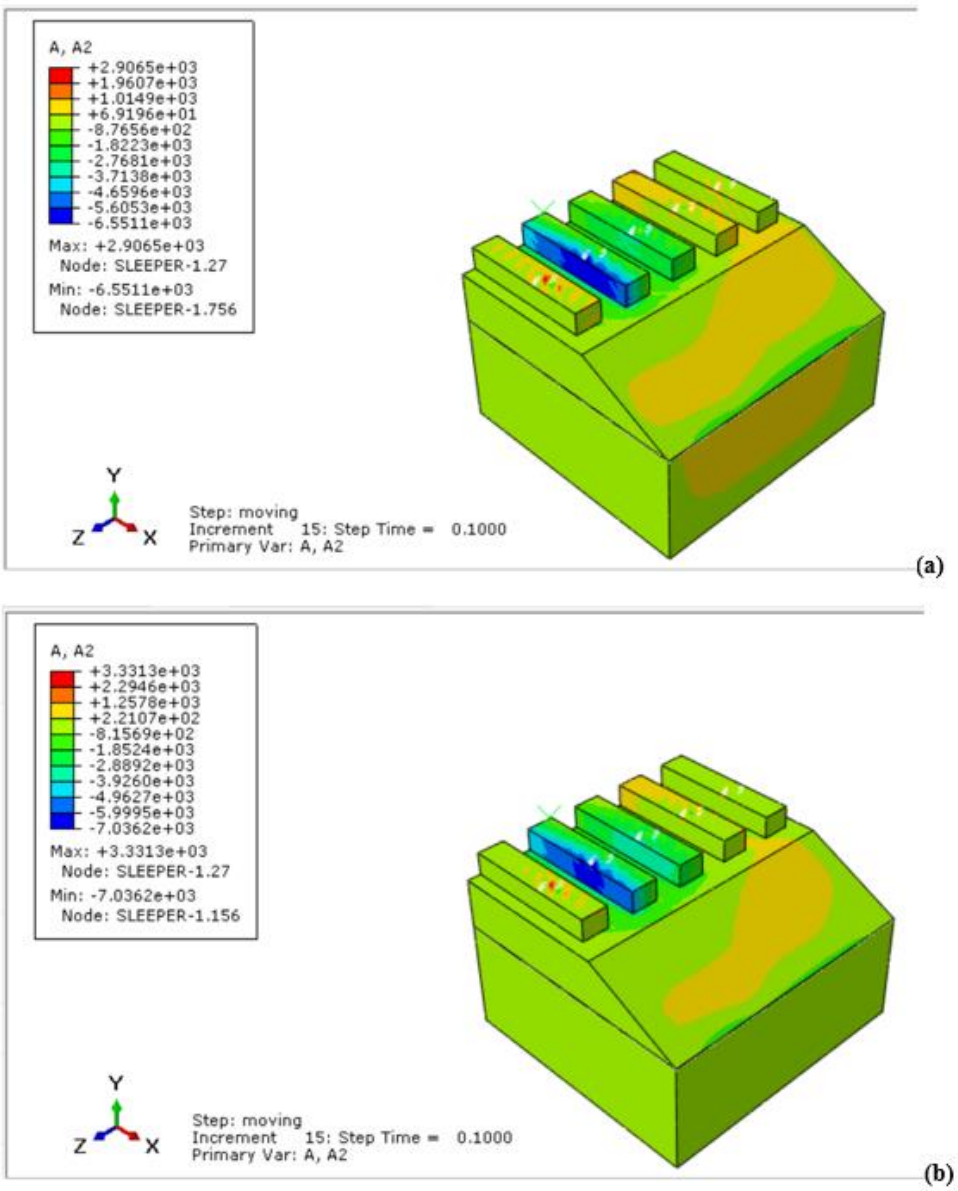

Figure B- 3 Sleeper vertical acceleration at rail pad stiffness of (a) 400 kN/mm and (b) 1000 kN/mm